Pharmacological Research 188 (2023) 106640

Contents lists available at ScienceDirect

Pharmacological Research

journal homepage: www.elsevier.com/locate/yphrs

Blocking the HGF-MET pathway induces resolution of neutrophilic inflammation by promoting neutrophil apoptosis and efferocytosis

Franciel Batista Felix [a], Julia Dias [a], Juliana Priscila Vago [b], Débora Gonzaga Martins [a], Vinícius Amorim Beltrami [a], Débora de Oliveira Fernandes [a], Anna Clara Paiva Menezes dos Santos [c], Celso Martins Queiroz-Junior [a], Lirlândia Pires de Sousa [d], Flávio Almeida Amaral [e], Frederico Marianetti Soriani [f], Mauro Martins Teixeira [e], Vanessa Pinho [a,*]

[a] Departamento de Morfologia, Instituto de Ciências Biológicas, Universidade Federal de Minas Gerais, Belo Horizonte, Brazil
[b] Experimental Rheumatology, Department of Rheumatology, Radboud Institute for Molecular Life Sciences, Radboud University Medical Center, Nijmegen, the Netherlands
[c] Departamento de Microbiologia, Instituto de Ciências Biológicas, Universidade Federal de Minas Gerais, Belo Horizonte, Brazil
[d] Departamento de Análises Clínicas e Toxicológicas, Faculdade de Farmácia, Universidade Federal de Minas Gerais, Belo Horizonte, Brazil
[e] Departamento de Bioquímica e Imunologia, Instituto de Ciências Biológicas, Universidade Federal de Minas Gerais, Belo Horizonte, Brazil
[f] Departamento de Genética, Ecologia e Evolução, Instituto de Ciências Biológicas, Universidade Federal de Minas Gerais, Belo Horizonte, Brazil

ARTICLE INFO

Keywords:
HGF
MET
Neutrophil apoptosis
Efferocytosis
Inflammation resolution
Annexin A1

ABSTRACT

Inflammation resolution is an active process that involves cellular events such as apoptosis and efferocytosis, which are key steps in the restoration of tissue homeostasis. Hepatocyte growth factor (HGF) is a growth factor mostly produced by mesenchymal-origin cells and has been described to act via MET receptor tyrosine kinase. The HGF/MET axis is essential for determining the progression and severity of inflammatory and immune-mediated disorders. Here, we investigated the effect of blocking the HGF/MET signalling pathway by PF-04217903 on the resolution of established models of neutrophilic inflammation. In a self-resolving model of gout induced by MSU crystals, HGF expression on periarticular tissue peaked at 12 h, the same time point that neutrophils reach their maximal accumulation in the joints. The HGF/MET axis was activated in this model, as demonstrated by increased levels of MET phosphorylation in neutrophils ($Ly6G^+$ cells). In addition, the number of neutrophils was reduced in the knee exudate after PF-04217903 treatment, an effect accompanied by increased neutrophil apoptosis and efferocytosis and enhanced expression of Annexin A1, a key molecule for inflammation resolution. Reduced MPO activity, IL-1β and CXCL1 levels were also observed in periarticular tissue. Importantly, PF-04217903 reduced the histopathological score and hypernociceptive response. Similar findings were obtained in LPS-induced neutrophilic pleurisy. In human neutrophils, the combined use of LPS and HGF increased MET phosphorylation and provided a prosurvival signal, whereas blocking MET with PF-04217903 induced caspase-dependent neutrophil apoptosis. Taken together, these data demonstrate that blocking HGF/MET signalling may be a potential therapeutic strategy for inducing the resolution of neutrophilic inflammatory responses.

1. Introduction

Inflammation is a protective physiological response acting on the elimination of the source of tissue perturbation (e.g., infection or injury), repairing tissue damage, and leading to the restoration of homeostasis [1–3]. Neutrophils exhibit crucial biological functions in the inflammatory response, contributing to the elimination of invading pathogens by the release of specialized granules and proinflammatory molecules [4,5]. Exacerbated recruitment of neutrophils and their extended survival in tissues are associated with failures in inflammation

* Correspondence to: Departamento de Morfologia, Instituto de Ciências Biológicas, Universidade Federal de Minas Gerais, Avenida Antônio Carlos 6627, Pampulha, 31270–901 Belo Horizonte, Minas Gerais, Brazil.
E-mail address: vpinho@icb.ufmg.br (V. Pinho).

https://doi.org/10.1016/j.phrs.2022.106640
Received 29 August 2022; Received in revised form 7 December 2022; Accepted 27 December 2022
Available online 7 January 2023

resolution [6,7], which contribute to the maintenance of tissue inflammatory responses leading to several human chronic diseases [8,9], including arthritis [10], cardiovascular diseases [11], obesity [12], asthma [13], COVID-19 [14], and cancer [15].

The success of the self-limited neutrophilic inflammatory response (restoring tissue homeostasis) is related to the interruption of neutrophil influx to the inflamed site. In addition, the shutdown of intracellular pathways implicated in cell survival leads to apoptosis of these cells and their subsequent clearance from inflamed tissue by macrophages in a process termed efferocytosis [16–18]. These processes are modulated by specialized pro-resolving mediators that efficiently collaborate to resolve inflammation, preventing cell and tissue necrosis and functional loss of the inflamed organ [14,19]. Accordingly, defects in apoptosis and efferocytosis potentiate the generation of several chronic inflammatory diseases, including gout, rheumatoid arthritis, asthma, neurodegenerative diseases, and atherosclerosis [20–24]. Therefore, knowledge of neutrophil prosurvival factors may be important for the development of therapeutic options for many neutrophilic inflammatory diseases in which resolution is compromised.

Hepatocyte growth factor (HGF) is a growth factor originally described as a potent mitogen for hepatocytes and mostly produced by cells of mesenchymal origin, which binds with high affinity to its receptor MET, also called c-MET or hepatocyte growth factor receptor. MET is a heterodimeric transmembrane tyrosine kinase receptor encoded by the *mesenchymal-epithelial transition factor* (*MET*) proto-oncogene and is mainly expressed by epithelial and endothelial cells [25–27]. When binding to HGF, MET undergoes dimerization and transphosphorylation of two tyrosine residues (Y1234 and Y1235) in the kinase domain followed by autophosphorylation of two tyrosine residues (Y1349 and Y1356) in the C-terminal region and subsequent recruitment of cytosolic effector proteins, leading to the activation of downstream signalling pathways involved in multiple cellular processes, including cell survival, proliferation, cellular recruitment, differentiation, tumorigenesis, and angiogenesis [28–31].

Aberrant MET activation has been found in a wide variety of solid tumours and facilitates uncontrolled cell proliferation, survival, and migration, resulting in highly aggressive tumours [32,33]. Moreover, several studies have already demonstrated that the HGF/MET axis is required for the progression and severity of different inflammatory and immune-mediated diseases, including rheumatoid arthritis [34], osteoarthritis [35], multiple sclerosis [36], COVID-19 [37] and colitis [38]. Indeed, HGF and MET have been identified in immune cells and may regulate their functions, including neutrophils, monocytes, macrophages, dendritic cells, and T and B lymphocytes [39–41]. Both mouse and human neutrophils constitutively express MET at low levels [39,42] but can be markedly upregulated by inflammatory stimuli such as tumour necrosis factor (TNF), lipopolysaccharide (LPS), phorbol myristate acetate (PMA), and formyl methionyl-leucyl-phenylalanine (fMLP) [43,44]. In addition, the HGF/MET axis is required for neutrophil adhesion to endothelial cells and transmigration during inflammatory processes in colitis, skin rash, peritonitis, and cancer [38,42,45].

Studies have demonstrated that the development of small molecular MET kinase inhibitors is an effective approach for modulating HGF/MET signalling in preclinical and clinical trials for cancer therapies [46,47]. PF-04217903 is a well-known tyrosine-kinase selective inhibitor of MET that competes with intracellular ATP and abrogates HGF-induced phosphorylation of MET and its downstream signalling. Of interest, PF-04217903 exhibited more than 1,000-fold selectivity for MET compared with other MET inhibitors [48,49]. In preclinical studies, PF-04217903 effectively blocked the survival and migration of a variety of cancer cells [50–52]. PF-04217903 has been investigated in phase I clinical studies in patients with papillary renal carcinoma [53]. Despite these studies in cancer, the potential effects of PF-04217903 in regulating neutrophil survival and the outcome of the inflammatory process have not yet been investigated. Thus, we hypothesized that pharmacological inhibition of the HGF/MET axis would be effective in activating pro-resolving programs in vitro and in vivo to control neutrophilic inflammation.

2. Materials and methods

2.1. Animals

Animal studies are reported in compliance with the recommendations of the law 11.794 from the National Council for Control of Animals Experimentation – CONCEA, Brazil. All animal care and experimental studies were approved by the Animal Ethics Council – CEUA– at Universidade Federal de Minas Gerais (UFMG), Brazil under protocol number 235/2016 and 204/2021. Male C57Bl/6 mice (8–10 weeks, 23 ± 2 g) were obtained from the Center of bioterism of UFMG and kept under standard environmental conditions (12 h light-dark cycles and 24 ± 2 °C). Food and water were provided ad libitum. All animals were randomly grouped resulting in equal number of sample sizes.

2.2. LPS-induced pleurisy model and treatment protocol

Mice received an intrapleural (i.pl.) injection of LPS (250 ng/cavity) or phosphate-buffered saline (PBS) as described previously [54]. For MET inhibition, PF-04217903 (AbMole Bioscience), a tyrosine-kinase selective inhibitor of the HGF receptor MET was used [49]. Then, at 4 h after LPS challenge, the mice received 40 mg/kg of PF-04217903 in carboxymethylcellulose (0.5% in saline) suspension or only the corresponding vehicle via oral gavage as reported previously [42]. Mice were euthanized (180 mg/kg of ketamine and 24 mg/kg of xylazine, i.p.) 4 h after PF-04217903 treatment and pleural wash was performed with 2 mL of PBS 1X. Total cell counts were determined using Turk's stain in a Neubauer chamber. Differential cell counting was performed using standard morphological criteria to identify leukocytes on cyto-centrifuge preparations (Shandon III) stained with May--Grünwald-Giemsa. The results are presented as the number of cells per pleural cavity.

2.3. Monosodium urate (MSU) crystals-induced gouty arthritis model and treatment protocol

Crystals of MSU were prepared using uric acid (Sigma-Aldrich - St. Louis MO, United States) as previously described [21,55]. Gouty arthritis was induced by an injection into the tibiofemoral left knee joint of mice under anesthesia (80:15 mg/kg ketamine:xylazine; i.p., Syntec, São Paulo, Brazil) with 100 μg of MSU crystals in 10 μL of sterile saline. Control group mice were challenged with sterile saline in the right knee joint. To assess the effects of MET inhibition on gout model, mice were treated with PF-04217903 (40 mg/kg) via oral gavage 12 h after MSU-challenge (at the peak of inflammation). To evaluate leukocyte apoptosis in the knee joint, a broad-spectrum caspase inhibitor zVAD-fmk (1 mg/kg, Tocris Bioscience, Minneapolis, MN, USA), was given intraperitoneally 15 min before PF-04217903 injection. The dosages of drugs were based on previous studies [42,56]. Of note, all treatment protocols were performed in a blinded manner. Mice were euthanized and the knee joint cavity was surgically exposed and washed with PBS/bovine serum albumin (BSA) 3% (2 ×5 μL) to collect the cells. The total number of leukocytes were determined using the Neubauer chamber after staining with Turk's solution. The differential counts were performed using standard morphologic criteria on a slide stained with May-Grunwald-Giemsa. Efferocytosis was assessed in cells collected from the knee cavity 6 h after PF-04217903 treatment by microscopy analysis of cytospin slides (500 cells/slide were counted) and determining the proportion of cells with efferocytic morphology (macrophage with apoptotic cells observed in their cytoplasm). Results are expressed as mean ± SEM of the percentage of macrophages with engulfed apoptotic neutrophil. Additionally, cells were surface-stained for 30 min with anti-F4/80-PECy7 antibody (eBioscience). Then, cells

were fixed for 10 min, permeabilized with permbuffer (Cytofix/Cytoperm Kit; BD Biosciences), and intracellularly stained with anti-Ly6G-BV421 antibody. Stained cells were acquired using BD FACSCanto II cell analyzer (BD Bioscience). Efferocytosis was evaluated by mean fluorescence intensity (MFI) of neutrophils ($Ly6G^+$) inside macrophages ($F4/80^+$). Periarticular tissues were collected from the joints for evaluation of cytokines, myeloreproxidase (MPO) activity and quantitation of mRNA expression by RT-qPCR.

2.4. Measurement of IL-1β and CXCL1

Mice were euthanized 18 h after MSU challenge and their periarticular tissues were collected and homogenized (Quiagen, Biotecnology Brazil Ltda, São Paulo, SP, Brazil) for 5 min in a protease inhibitor solution [NaCl (0.4 M); Tween 20 (0.05% w/v); BSA (0.5% v/v); phenylmethylsulfonyl fluoride (PMSF) (0.1 mM); benzethonium chloride (0.1 mM); EDTA (10 mM); and aprotinin (20 IU)] in PBS. The samples were centrifuged for 10 min at 10,000 rpm at 4 °C. The concentration of IL-1β and CXCL1 was measured by enzyme-linked immunosorbent assay (ELISA) in the supernatants of the homogenates and using commercially available antibodies according to the procedures supplied by the manufacturer (R&D Systems, Minneapolis, MN, United States).

2.5. Measurement of MPO activity

Neutrophil recruitment into the knee joint was evaluated via the quantification of the myeloperoxidase (MPO) enzyme activity as previously described [57]. Briefly, the pellet from samples homogenized for cytokines measurements, were homogenized with 0.05 M NaH2PO4 containing 0.5% of hexadecyltrimethyl-ammoniumbromide (HETAB, Sigma-Aldrich). Samples were frozen 3 times in liquid nitrogen and centrifuged 10,000 rpm, 10 min at 4 °C, to collect the supernatant for MPO assay. The assay used 3,3',5,5'-tetramethylbenzidine (TMB, Sigma-Aldrich Corp., St. Louis, MO, USA) and was quantified at 450 nm in a spectrophotometer. Results are expressed as absorbance.

2.6. Evaluation of hypernociception

Mice were individually placed in acrylic cages (12 ×10 x 17 cm in height) with a wire-grid floor, in a noised controlled room, for 60 min. After this time, exploratory behavior manifestation was abrogated, and all mice remained quiet allowing for nociceptive response evaluation. To identify the withdrawal threshold, an electronic von Frey algesimeter (INSIGHT Instruments, Ribeirão Preto, SP, Brazil) was applied according to the methods previously used [58]. In brief, using a hand-held force transducer, fitted with a polypropylene tip (4.15 mm), the observer applied a vertical and constant force in the central plantar surface of the mice paw. This procedure was intended to produce an articular mechanical stimulus for knee flexion. The sufficient force in grams (g) to trigger a paw withdrawal movement, the characteristic aversive behavior to avoid the incident stress, was recorded by an electronic component of the apparatus. The withdrawal threshold was calculated by replicating the procedure in triplicate for each mouse (and averages were expressed in absolute values). The nociceptive response was observed at 18 h after MSU knee injection and conducted in a blinded experimental condition.

2.7. Histology and immunohistochemistry

Tibiofemoral joint samples were collected and fixed in 10% (v/v) buffered formalin (pH 7.4), decalcified for 30 days in 14% EDTA. Tissues were included in paraffin, sectioned (5 mm) and stained with Hematoxylin-Eosin (H&E). Then, H&E sections were examined and scored by a pathologist in a blinded manner for the following parameters: severity of synovial hyperplasia, intensity of inflammatory infiltrate, vascular hyperemia, and changes in tissue architecture. The grades were summed to obtain a histopathological score (ranging from 0 to 12) as described [59]. Additionally, the sections were incubated with anti-AnxA1 (1:400; Invitrogen, Thermo Fisher Scientific, Waltham, MA, USA), followed by a biotinylated secondary antibody, and the color was developed using DAB (3,3′-diaminobenzidine) (Sigma, Sigma-Aldrich). The sections were counterstained with hematoxylin, mounted, and examined using a Motic microscope (Carl Zeiss, Gottingen, Germany).

2.8. Human neutrophil isolation and culture

Neutrophils were isolated from the peripheral blood of healthy donors as described elsewhere [60]. Briefly, blood was collected into ethylenediamine tetraacetic acid (EDTA) and was separated through a double-density gradient using Histopaque 10,771 and 11,191 (both Sigma-Aldrich). After polymorphonuclear cell isolation and wash, contaminating erythrocytes were removed by hypotonic lysis. Neutrophil isolates were approximately 90% pure as confirmed by morphological appearance using light microscopy. Cells were resuspended at 2×10^5/mL in RPMI-1640 medium (Sigma-Aldrich), cultured at 37 °C with 5% CO2, and treated with PF-04217903 (30 μM) for 1 h followed by further incubation with LPS (1 μg/mL), recombinant human HGF (ImmunoTools, 100 ng/mL) or MSU (100 μg/mL) according to the experimental setting. To neutrophil apoptosis analyses, zVAD-fmk (15 μM) was added 15 min prior to PF-04217903. Incubation time was determined based on previous publications [56,60,61]. All subjects enrolled gave their informed consent for inclusion in the study. The study was conducted in accordance with the Declaration of Helsinki, and the protocol was approved by the Ethics Committee of Institutional Review Board Project number CAAE – 32806720.0.0000.5149.

2.9. Assessment of Leukocyte apoptosis

Apoptosis was assessed morphologically, as described [60]. Briefly, 5×10^4 cells collected 8 h after LPS administration or 18 h after MSU injection were cyto-centrifuged, fixed, and stained with May–-Grünwald–Giemsa and counted using oil immersion microscopy (×100 objective) to determine the proportion of cells with distinctive apoptotic morphology in a blind manner. Of note, cells were considered apoptotic when exhibited chromatin condensation, nuclear fragmentation, and formation of apoptotic bodies (Poon et al., 2014). At least 300 cells were counted/slide, and results are expressed as mean ± SEM of the percentage of cells with apoptotic morphology. Apoptosis was also evaluated by flow cytometry using BD FACSCanto II cell analyzer (BD Bioscience) and analyzed using FlowJo Software (Tree Star Inc., USA). For this, cells were harvested 6 h after LPS administration or 15 h after MSU injection of mice. Then, cells were surface-stained for 30 min with the anti-LY6G antibody (BV421-BD Bioscience, San Jose, CA, USA) or anti-F4/80 antibody (PE-Cy7-eBioscience, San Diego, CA, USA) and then labeled with annexin-V-APC and propidium iodide (PI), as an index of loss of nuclear membrane integrity (Annexin-V Apoptosis Detection Kit; BD PharmingenTM; United States). For in vitro neutrophil apoptosis analyses, human neutrophils were collected according to the experimental setting, and apoptosis was evaluated biochemically (2 h after PF-04217903 treatment) by flow cytometry or by morphological examination (6 and 12 h after PF-04217903 treatment or LPS/HGF stimulation, respectively), as described above.

2.10. Mice blood cells isolation

Under anesthesia, mice were euthanized by cervical dislocation, and blood samples were collected from the abdominal cava vein in 10% heparin and diluted in an equal volume of PBS 0.5% BSA. Next, erythrocytes were removed by hypotonic lysis. Cells were washed in PBS 0.5% BSA, counted, and resuspended according to the experimental

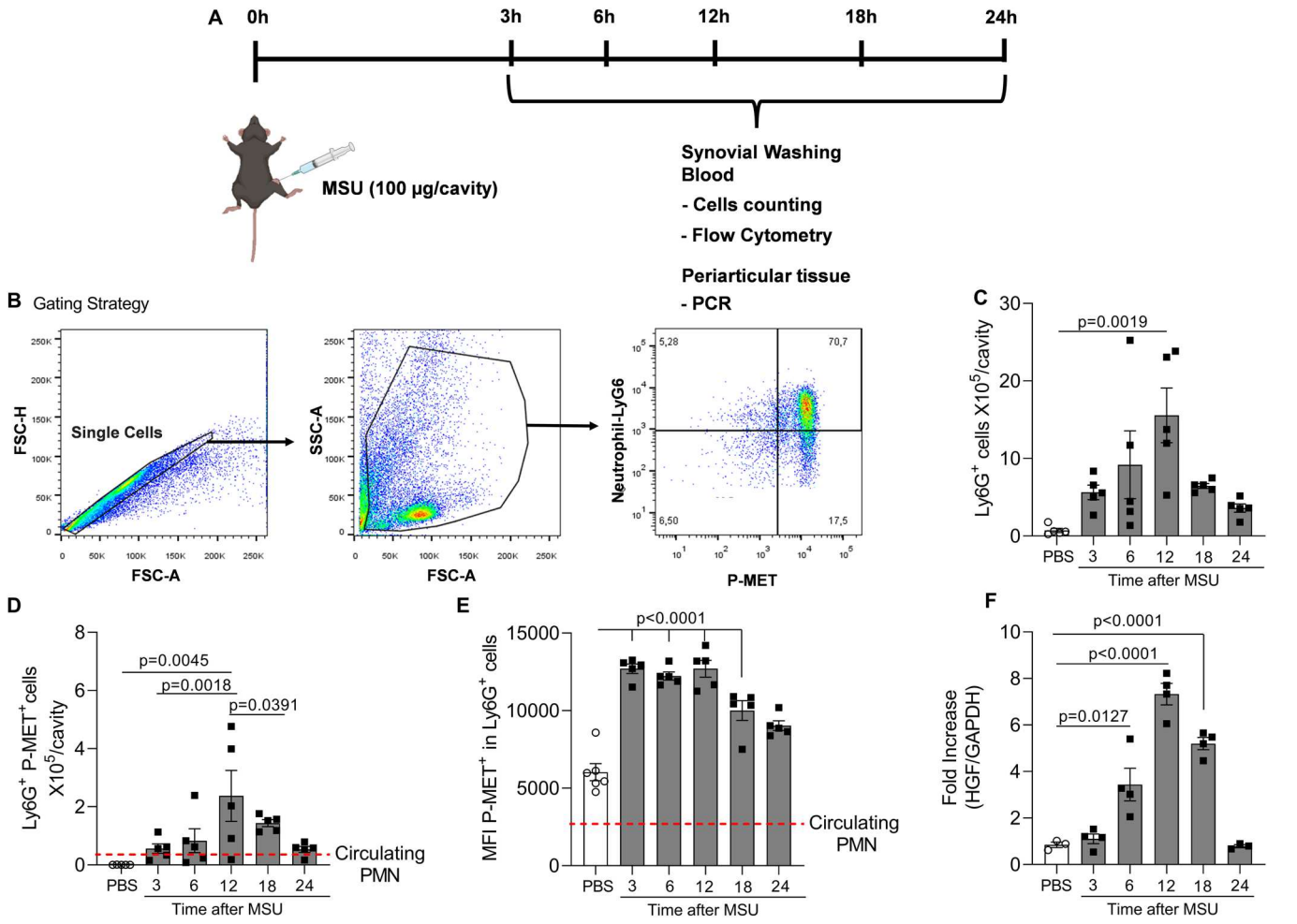

Fig. 1. Time-course of HGF/MET expression in MSU-induced gout. Mice were injected with MSU crystals (100 µg/10 µL of PBS) into the tibiofemoral joint. Control mice were injected with phosphate-buffered saline (PBS) (10 µL). Cells were harvested from articular cavity 3, 6, 12, 18, and 24 h after MSU challenge. Cells were surface-stained with anti-Ly6G and then intracellularly stained with anti-P-MET antibody and were analyzed by flow cytometry (A). Representative dot plots of gating strategy are presented (B) and results are expressed as the number of $Ly6G^+$ cells/cavity (C), $Ly6G^+$ $P\text{-}MET^+$ cells/cavity (D) and mean fluorescence intensity (MFI) of $P\text{-}MET^+$ on positive $Ly6G^+$ cells (E). HGF quantification was assessed by Real-time PCR in periarticular tissue (F). Results are shown as the mean ± SEM of n = 4–5 mice in each group. Significance was calculated using one-way ANOVA followed by Tukey's test. The specified p-values are shown in the figure.

settings.

2.11. Flow cytometry analysis for leukocyte populations and intracellular levels of phospho-MET, Annexin A1, cleaved caspase-3 and Bcl-xL

Inflammatory cells harvested from the synovial cavity of mice at different time points (3, 6, 12, 18 and 24 h after MSU challenge) or blood cells were analyzed for MET phosphorylation (P-MET) by flow cytometry. Briefly, populations of macrophages and neutrophils were surface-stained for 30 min with anti-Ly6G antibody (BV421-BD Bioscience) or anti-F4/80 antibody (PE-Cy7-eBioscience). After being stained for surface markers, cells were fixed by incubating with 2% formaldehyde for 20 min. Then, cells were washed and permeabilized with permeabilization buffer (True-Phos™ Perm Buffer, BD Bioscience) for 30 min. After permeabilization, cells were intracellular-stained for 1 h with the anti-phosphorylated-MET antibody (#3077; Cell Signaling Technology, Beverly, MA, USA, 1:200) and anti-rabbit secondary antibody (Alexa 488-APC; BD Biosciences, 1:200). Negative controls were cells stained only with fluorochrome-bound secondary antibodies anti-rabbit. Stained cells were acquired using BD FACSCanto II cell analyzer (BD Bioscience) and analyzed using FlowJo Software (Tree Star Inc., USA). $P\text{-}MET^+$ $Ly6G^+$ neutrophil population was analyzed. In addition, the frequency of macrophages ($F4/80^+$) and neutrophils ($Ly6G^+$) positive for Annexin A1 (AnxA1) was verified in cells obtained from articular lavage 6 h after PF-04217903 treatment. *In vitro* P-MET analysis was performed in human neutrophils treated with PF-04217903 (30 µM) for 1 h followed by further incubation with LPS (1 µg/mL) and HGF (100 ng/mL) or MSU (300 µM) for 2 h by flow cytometry as described above. Furthermore, human neutrophils were immunolabeling with anti-cleaved caspase-3 (Asp175) (Clone 5A1E; #9664; Cell Signaling Technology, 1:400) and anti-B-cell lymphoma-extralarge (Bcl-xL) antibody (Clone 54H6; #2764; Cell Signaling Technology, 1:400), and anti-rabbit secondary antibody (Alexa 488-APC; BD Biosciences, 1:200).

2.12. Quantitation of mRNA expression by RT-qPCR

Total RNA was extracted and isolated from periarticular tissue at different time points (3, 6, 12, 18 and 24 h after MSU-injection) using TRIzol Reagent (Invitrogen Life Technologies Corporation- Carlsbad, CA, USA) according to the manufacturer's instructions. Total RNA purity was determined using a Nanodrop 1000 spectrophotometer (Thermo Scientific- Waltham, MA, USA). A mix containing the reserve transcriptase, SuperScript III, ribonuclease recombinant inhibitor (RNAse Out; Invitrogen Life Technologies Corporation) and dithiothreitol (DTT; 1 mM) were used for reverse transcription of 500 ng of isolated total RNA into cDNA. The reverse transcription step was carried out in

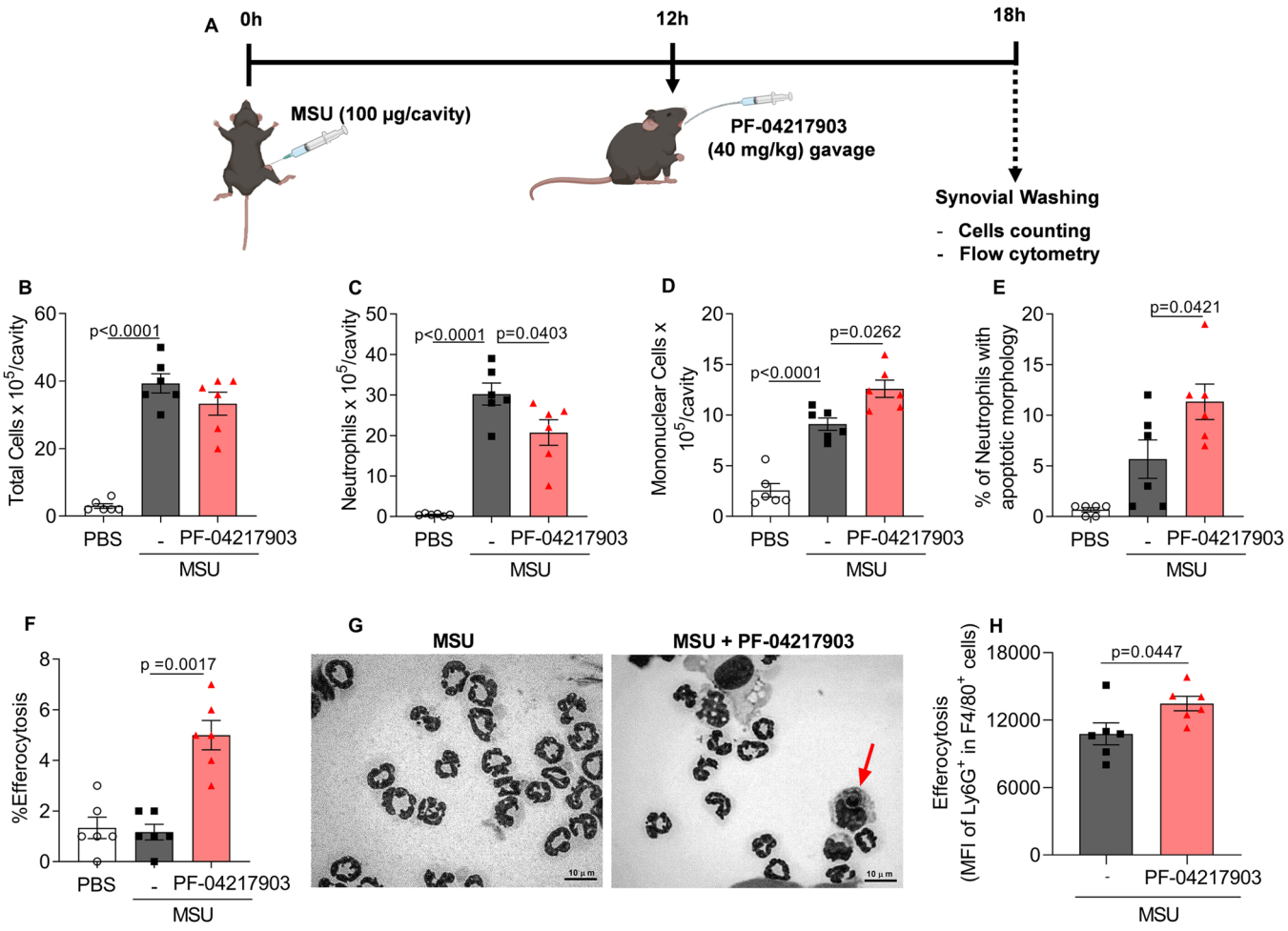

Fig. 2. Inhibition of the HGF/MET pathway in MSU-induced gout. Mice were injected with MSU crystals (100 µg/10 µL of PBS) into the tibiofemoral joint. Control mice were injected with phosphate-buffered saline (PBS) (10 µL). Mice were treated with PF-04217903 (40 mg/kg) by gavage 12 h post-MSU challenge (A). Cells were harvested from the articular cavity at 6 h post-treatment and the number of total cells (B), neutrophils (C), mononuclear cells (D), apoptotic neutrophils (E) and efferocytosis (F) were morphologically identified in cytospin slides counting. Representative figures of apoptotic neutrophils ingested by macrophages (arrows) are shown (G). Magnification × 100. Flow cytometry analysis was performed to assess efferocytosis in cells from the articular cavity (H). Knees were washed 18 h post-MSU injection and cells were surface-stained with anti-F4/80 for macrophages and then intracellularly stained with anti-Ly6G for neutrophils. Results are demonstrated as mean fluorescence intensity (MFI) of $Ly6G^+$ on positive $F4/80^+$ cells. Results are shown as the mean ± SEM of n = 6 in each group. Significance was calculated using one-way ANOVA followed by Tukey's test. The specified p-values are shown in the figure.

duplicate, and the total RNA concentration was similar in every sample. For quantitative Real-time qPCR the Power SYBR Master Mix reagent (Invitrogen Life Technologies Corporation) and initiators pars (Integrated DNA Technologies- Coralville, IA, EUA) plus cDNA were placed into a 96-well plate in duplicate in a total reaction volume of 10 µL, using the StepOneTM System (Applied Biosystems, Waltham, MA, EUA) in programmed reaction: initial heating at 95°C for 10 min, following by 40 cycles at 95°C for 60 s and 48°C for 1 min. The data were analyzed using StepOneTM System software and processed by the 2ˆ-ΔCT method. This method directly uses the CT (threshold cycle) information generated from a qPCR system to calculate relative gene expression in target and reference samples, using a reference gene to normalize the RT-qPCR. The following primers were used: HGF forward, 5'-TGGTCCTGAAGGCTCAGACT5'; HGF reverse 5'-CAGGATTGCAGGTC-GAGCAA-3'; glyceraldehyde-3-phosphate dehydrogenase (GAPDH) forward, 5'-AGAAGACTGTGGATGGCCCC-3', GAPDH reverse, 5'-TGACCTTGCCCA CAGCCTT-3'. Primer and probe sequences were checked with BLAST™ software. GAPDH was used as a reference gene control and results were expressed as fold increase compared to the PBS-treated control groups.

2.13. Thymocytes preparation, labeling, and apoptosis

Thymocytes were isolated from the thymus of male C57Bl/6 mice using established protocols [62]. Briefly, thymocytes were labeled with carboxyfluorescein diacetate succinimidyl ester (CFSE, 2.5 µM, Life Technologies). Next, CFSE-labeled thymocytes were stimulated with staurosporine (1 µM, Sigma-Aldrich) for the induction of apoptosis for 4 h at 37 °C under light protection. The percentage of apoptosis was performed by preparing cytospin slides and determining the proportion of cells with apoptotic morphology and > 85% were apoptotic.

2.14. In Vivo efferocytosis assay

To investigate the direct impact of the HGF/MET pathway inhibition on the efferocytic ability of macrophages, efferocytosis was assessed by flow cytometry in macrophages from peritoneal exudate, as reported by [56,63,64]. Briefly, mice received an intraperitoneal (i.p.) injection of zymosan 0.1 mg/cavity. After 90 h, mice were treated with PF-04217903 (40 mg/kg, via oral gavage) and 6 h later received an i.p. injection containing apoptotic thymocytes labeled with CFSE (3×10^6 cells/cavity). Mice were euthanized 30 min after injection of the apoptotic thymocytes, and cells were recovered from the peritoneal

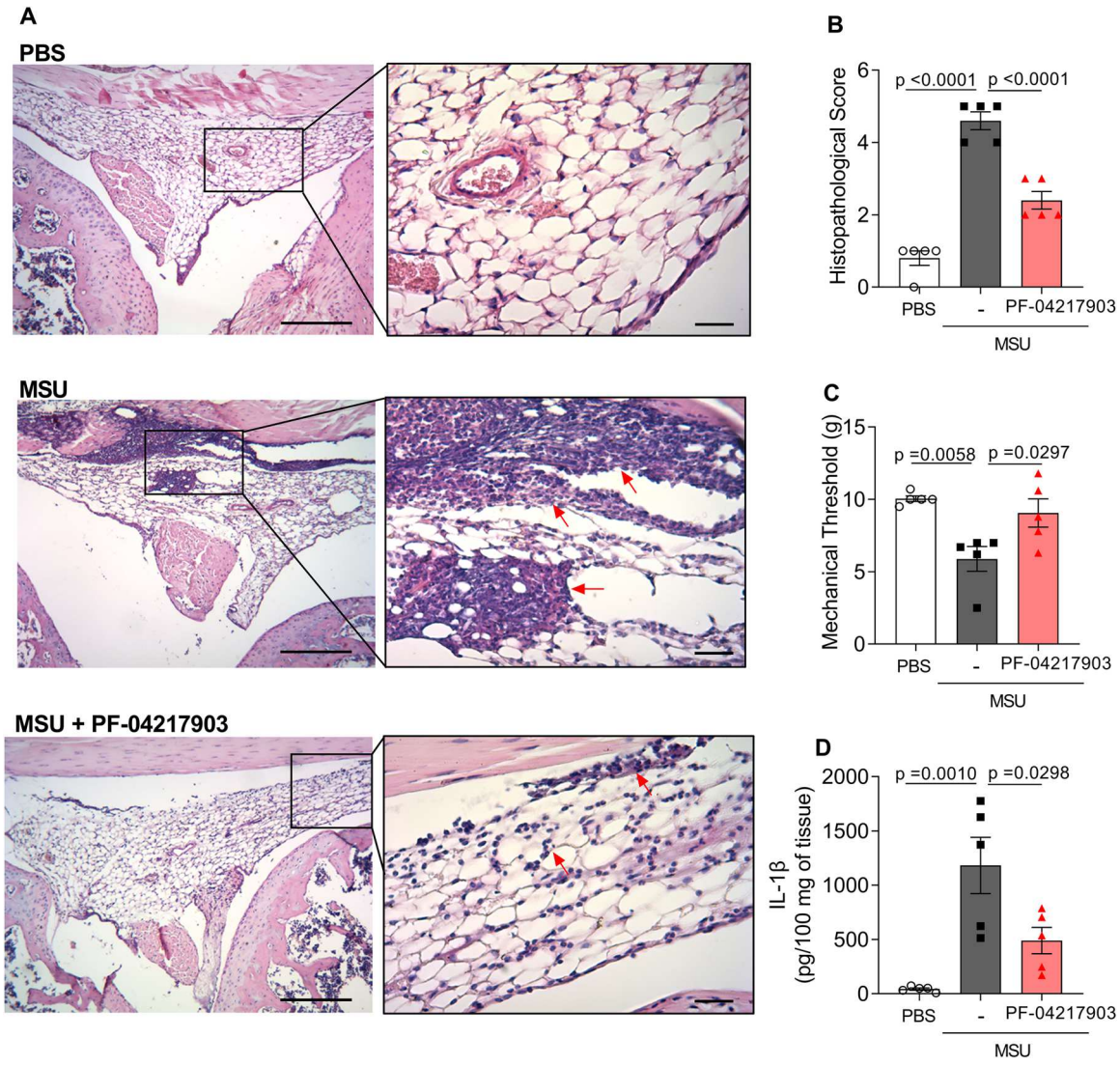

Fig. 3. Inhibition of the HGF/MET pathway on tissue damage and hypernociceptive response triggered by MSU. Mice were injected with MSU crystals (100 μg/10 μL of PBS) into the tibiofemoral joint. Control mice were injected with phosphate-buffered saline (PBS) (10 μL). Mice were treated with PF-04217903 (40 mg/kg) by gavage at 12 h post-MSU challenge. At 6 h after treatment knees were collected for histopathological analysis. Representative histological slide in H&E staining is represented (A — arrows indicate the intensity of inflammatory infiltrate). Histopathological score quantification of knee joint samples (B). IL-1β levels in the periarticular tissue homogenate were evaluated by ELISA (C). The mechanical hypernociception was evaluated by an electronic von Frey algesimeter 18 h after MSU challenge (D). Results are shown as the mean ± SEM of n = 5 in each group. Significance was calculated using one-way ANOVA followed by Tukey's test. The specified p-values are shown in the figure.

cavity and incubated for labeling with anti-F4/80 antibody for 20 min. Stained cells were acquired using BD FACSCanto II cell analyzer and analyzed using FlowJo Software. The results of flow cytometry are presented as the frequency of F4/80$^+$/CFSE$^+$ cells and MFI of apoptotic thymocytes (CFSE$^+$) inside macrophages (F4/80$^+$). Efferocytosis was also performed by morphological examination.

2.15. Statistical analysis

The data and statistical analysis complied with the recommendations of the British Journal of Pharmacology on experimental design and analysis [65]. Studies were designed to generate groups of equal size, using randomization and blinded analysis. Data were tested for normality using the Shapiro–Wilk test, and statistical significance was determined using GraphPad Prism 8 software (GraphPad Software Inc., CA, USA). All results are expressed as mean ± SEM. Data were analyzed by one-way ANOVA, followed by the Tukey's post hoc test. When only two groups were evaluated, Student's t test was used. A value of $p < 0.05$ was considered statistically significant.

3. Results

3.1. HGF/MET is expressed in neutrophils during MSU crystal-induced gout

Initially, we measured HGF and P-MET in an MSU-induced acute gout model, which is a model for studies of neutrophil lifespan at sites of inflammation [21,55,60]. MSU crystals were injected into the tibiofemoral joint, and synovial exudates were evaluated by flow cytometry at 3, 6, 12, 18, and 24 h (Fig. 1 A). Representative dot plots for gating strategy are shown in Fig. 1B. As expected, mice injected with MSU displayed robust influx of leukocytes, mainly neutrophils (Ly6G$^+$), into the knee joint during the first 3 h and peaked at 12 h, which gradually decreased thereafter (Fig. 1 C). P-MET expression in Ly6G$^+$ infiltrating cells was detectable early at 3 h and persisted up to 18 h after administration of MSU (Fig. 1D, E). Of note, Ly6G$^+$ circulating cells from

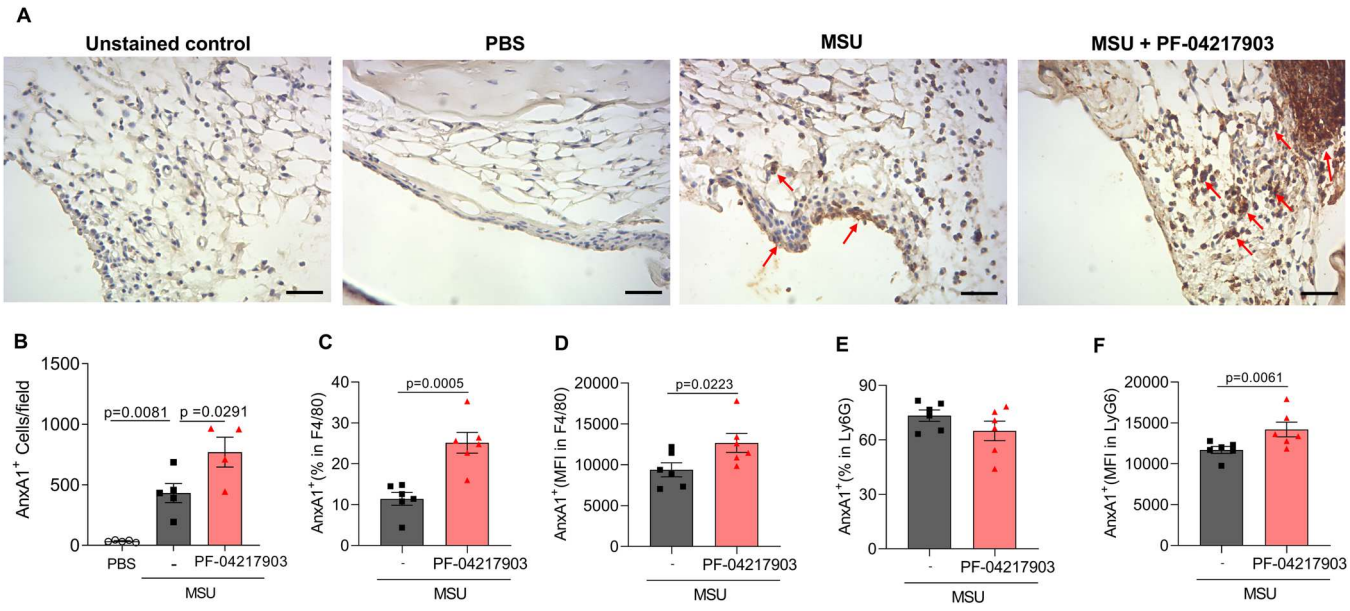

Fig. 4. Inhibition of the HGF/MET pathway on Annexin A1 expression in MSU-induced gout. Mice were injected with MSU crystals (100 μg/10 μL of PBS) into the tibiofemoral joint. Control mice were injected with phosphate-buffered saline (PBS) (10 μL). Mice were treated with PF-04217903 (40 mg/kg) by gavage at 12 h post-MSU challenge. At 6 h after treatment knees were collected for immunohistochemistry analysis for Annexin A1 (AnxA1). Samples were quantified as the average of $AnxA1^+$ cells in five independent fields per tissue at 40x. Representative images of positive AnxA1 cells (arrow) are shown in (A) and score is graphed in (B). Flow cytometry analysis was performed to assess AnxA1 in cells from the articular cavity. Knees were washed 18 h post-MSU injection and cells were surface-stained with anti-F4/80 for macrophages and anti-Ly6G for neutrophils and then intracellularly stained with anti-AnxA1 antibody. Results are expressed as the frequency and mean fluorescence intensity (MFI) of $AnxA1^+$ in $F4/80^+$ (C, D) and $LyG6^+$ cells (E, F), respectively. Results are shown as the mean ± SEM of n = 4–6 in each group. Significance was calculated using one-way ANOVA followed by Tukey's test. The specified p-values are shown in the figure.

healthy mice did not express high levels of $P\text{-}MET^+$ (Fig. 1D, E), indicating that elevated HGF/MET pathway activation in gout is only exhibited by cells in the inflamed joint. Interestingly, HGF mRNA expression levels in the joint peaked at 12 h, displaying a similar pattern as the neutrophil accumulation kinetics during articular inflammation (Fig. 1 F). In summary, these data indicated that the neutrophilic HGF/MET pathway is activated during the course of MSU crystal-induced gout.

3.2. Blocking the HGF/MET pathway promotes resolution of inflammatory response

Considering that the HGF/MET pathway was upregulated during the articular inflammation, we aimed to determine whether blocking MET activation using PF-04217903, a MET tyrosine-kinase inhibitor [49], may contribute to the cessation of inflammation by the induction of the inflammation resolution program. Thus, mice were injected into the tibiofemoral joint with MSU crystals and treated with PF-04217903 via oral gavage at the peak of inflammation (12 h after MSU injection), and 6 h later, synovial exudate was collected and analysed (Fig. 2 A). The treatment of mice with PF-04217903 had no effect on the number of total infiltrating leukocytes (Fig. 2B), although decreased neutrophil accumulation in the synovial cavity was observed (Fig. 2 C). PF-04217903 treatment increased the number of mononuclear cells (Fig. 2D) and neutrophils with apoptotic morphology (Fig. 2E). In addition to increased apoptosis, PF-04217903 also increased the efferocytosis rates of apoptotic neutrophils by macrophages (Fig. 2F-G), which was further confirmed by flow cytometry (Fig. 2H, see supplementary Fig. 1 A for gating strategy). Similar findings were obtained when PF-04217903 was administered to LPS-induced pleurisy mice (Supplementary Fig. 2), a self-resolving model of acute neutrophilic inflammation [54,66].

Collectively, these results demonstrated that the pharmacological blockade of the HGF/MET axis contributes to inflammation resolution by enhancing neutrophil apoptosis and efferocytosis in the joint.

3.3. Blocking the HGF/MET pathway reduces tissue damage and the hypernociceptive response triggered by MSU crystals

To further elucidate the effect of the resolution of inflammation triggered by HGF/MET blockage on the gout model, we evaluated the effect of PF-04217903 treatment on joint tissue damage and pain 18 h after MSU injection. PF-04217903 reduced histopathological score, as demonstrated by H&E staining (arrows indicate the intensity of inflammatory infiltrate) (Fig. 3 A) and morphometric analysis (Fig. 3B). Details of histopathological score are shown in supplementary figure 3.

To assess the role of the HGF/MET pathway in the degree of articular dysfunction triggered by MSU crystals, the effect of PF-04217903 on mechanical hypernociception was analysed. Treatment with PF-04217903 ameliorated joint dysfunction by increasing the paw withdrawal threshold in response to mechanical stimulation in the inflamed limb (Fig. 3 C) and concomitantly reduced periarticular IL-1β levels (Fig. 3D), which is a key proinflammatory cytokine known to be upregulated during neutrophil-dependent hypernociception [55,67].

Taken together, these findings indicate that the pharmacological inhibition of the HGF/MET pathway by PF-04217903 improved mechanical hypernociception and tissue architecture in mice with gout, accompanied by a reduction of mediators of joint inflammation.

3.4. Blocking HGF/MET axis results in increased Annexin A1 levels

Given that the Annexin A1 (AnxA1) has well-known pro-resolving actions including induction of neutrophil apoptosis and efferocytosis [68,69], we next investigated whether AnxA1 could be associated with the resolution properties of PF-04217903 in the joint inflammation. Interestingly, a significant increased expression of AnxA1 was noted in the periarticular tissue of mice treated with the HGF/MET axis blocker (Fig. 4A-B). Supporting the immunohistochemistry findings, flow cytometry analysis showed that macrophages ($F4/80^+$) and neutrophils ($Ly6G^+$) from the synovial cavity of PF-04217903-treated mice had increased intracellular levels of AnxA1 in comparison to cells from the

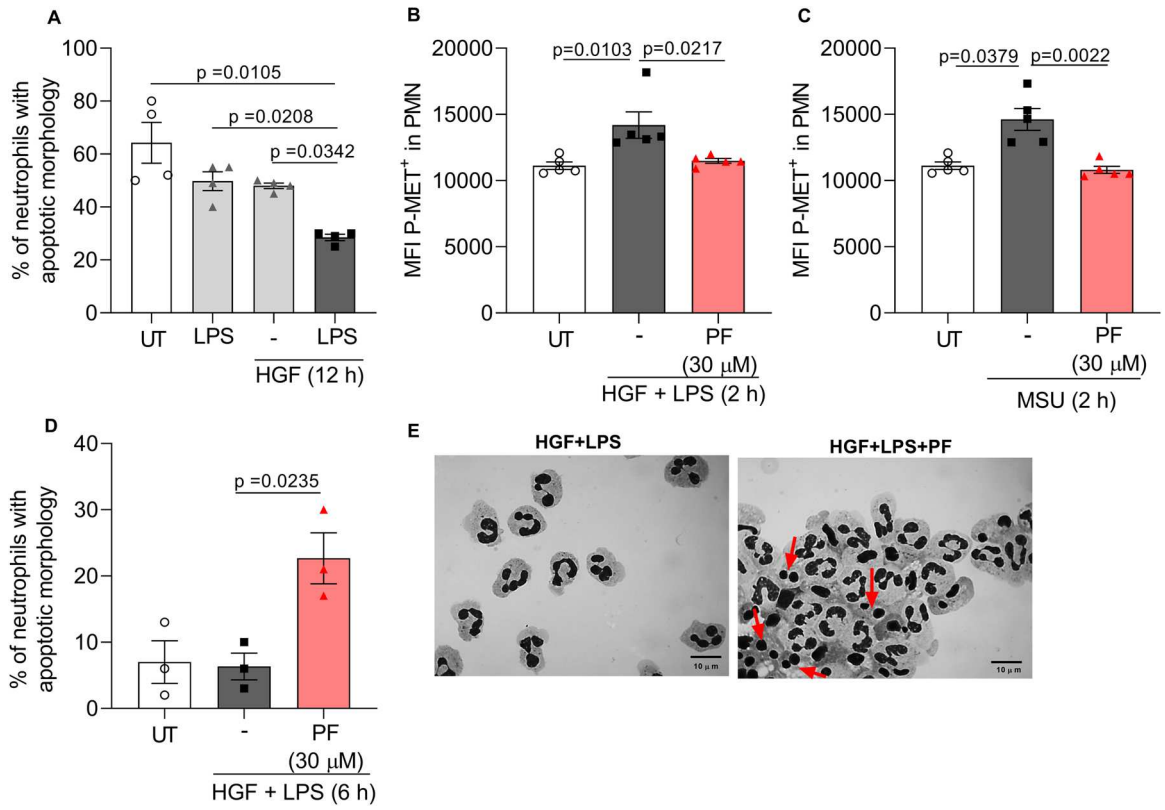

Fig. 5. Inhibition of the HGF/MET pathway on human neutrophil survival. Neutrophils were isolated from the human peripheral blood and cultured in the absence or presence of human recombinant HGF (100 ng/mL), LPS (1 μg/mL), or both (HGF+LPS) for 12 h. Morphological examination by cytospin slides counting was performed to identify apoptotic neutrophils (A). Human neutrophils were treated with PF-04217903 (30 μM) for 1 h followed by further incubation with LPS (1 μg/mL) and HGF (100 ng/mL) or MSU crystals (100 μg/mL) for 2 h, and then were stained intracellularly with the anti-P-MET antibody and flow cytometry was performed. Results are demonstrated as mean fluorescence intensity (MFI) of P-MET+ on human neutrophil (B, C). Apoptosis was morphologically identified in cytospin slides counting 6 h after LPS/HGF stimulation (D). Representative figures of apoptotic neutrophils (arrows) are shown (E). Magnification x100. The experiment is a representative of three independent experiments performed in biological triplicates and is shown as the mean ± SEM, significance was calculated using one-way ANOVA followed by Tukey's test. The specified p-values are shown in the figure.

vehicle group (Fig. 4 C, D, and F). Changes in the frequency of $Ly6G^{+}AnxA1^{+}$ cells (Fig. 4E) were not observed. Supplementary Fig. 1B display the gating strategy for these analyzes. Altogether, these results demonstrated that HGF/MET blockage is related to increased AnxA1 expression in the joint, which may contribute to the resolution of inflammation.

3.5. Blocking the HGF/MET axis impairs neutrophil survival by inducing apoptosis

Next, we investigated the relevance of the HGF/MET pathway to lifespan of human peripheral blood-derived neutrophil. Thus, human neutrophils were cultured in the absence or presence of LPS (1 μg/mL) and recombinant human HGF (100 ng/mL), and the percentage of apoptotic cells was then evaluated by morphological examination at 12 h after incubation, a time point at which a significant population had undergone spontaneous apoptosis in culture [61]. Neutrophils stimulated with both LPS and HGF exhibited an extended lifespan (Fig. 5 A), as evidenced by a lower rate of apoptosis (~30%), compared with cells exposed to only LPS or HGF alone (~50%) and unstimulated cells (~70%). By flow cytometry, we observed that the LPS+HGF stimulation enhanced the phosphorylation of MET in human neutrophils after 2 h compared with unstimulated cells (Fig. 5B) (see supplementary Fig. 4 A for gating strategy). In agreement with the in vivo findings, P-MET was also observed in MSU crystal-stimulated human neutrophils (Fig. 5 C). Most importantly, PF-04217903 abrogated LPS+HGF or MSU-induced P-MET in neutrophils (Fig. 5B, C), which was accompanied by an increase in the number of apoptotic cells 6 h after treatment, as shown by morphological criteria (Fig. 5D, E). Together, these findings revealed a crucial role of HGF and MET phosphorylation in regulating neutrophil lifespan.

3.6. Caspase-dependent neutrophil apoptosis is required for inflammation resolution induced by PF-04217903

Because neutrophil apoptosis was associated with the blocking the HGF/MET axis in vivo and in vitro, we next investigated whether zVAD-fmk, a broad-spectrum caspase inhibitor, could block the effects of PF-04217903 treatment (Fig. 6 A). Consistent with the previous data, PF-04217903 treatment did not significantly alter the number of total leukocytes in the synovial cavity (Fig. 6B), while a reduction in the number of neutrophils was observed (Fig. 6 C). Mononuclear cell numbers were not affected (Fig. 6D). In addition, a reduction in the accumulation of neutrophils in periarticular tissue, as measured by the myeloperoxidase (MPO) assay (Fig. 6E), was observed concomitantly with decreasing levels of the chemokine CXCL1 (Fig. 6 F). Of note, P-MET inhibition by PF-04217903 treatment demonstrated an increased percentage of apoptotic neutrophils in the knee cavity, as demonstrated by morphological analysis (Fig. 6 G) or when apoptosis was evaluated biochemically using labelled annexin-V by flow cytometry analysis (Fig. 6H, I). See supplementary Fig. 5 A for gating strategy. Interestingly, PF-04217903 treatment did not induce macrophage apoptosis (Supplementary Fig. 6). Most importantly, PF-04217903 effects were all prevented when mice were pretreated with zVAD-fmk (Fig. 6B-I). Notably,

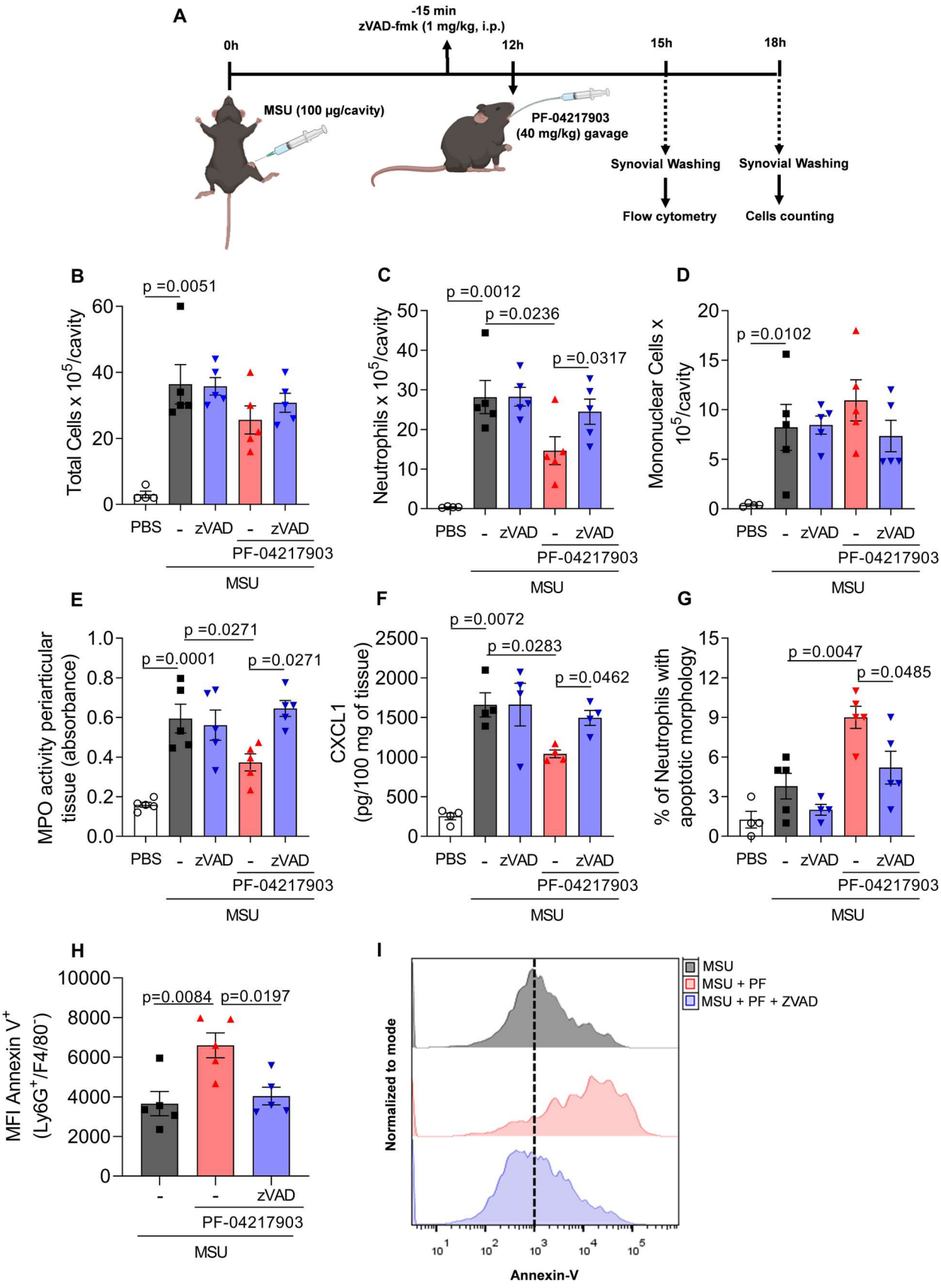

(caption on next page)

Fig. 6. Inhibition of HGF/MET pathway during MSU-induced gout and effect of zVAD-fmk. Mice were injected with MSU crystals (100 μg/10 μL of PBS) into the tibiofemoral joint. Control mice were injected with phosphate-buffered saline (PBS) (10 μL). Mice were treated with PF-04217903 (40 mg/kg) by gavage at 12 h post-MSU challenge. The pan-caspase inhibitor zVAD-fmk (1 mg/kg, i.p.) was given 15 min before PF-04217903 treatment (A). Cells were harvested from the articular cavity 6 h post-treatment and the number of total cells (B), neutrophils (C) and mononuclear cells (D) were evaluated by cytospin counting. Neutrophil accumulation on the periarticular tissue was measured by the activity of myeloperoxidase (E). CXCL1 levels were quantified by ELISA in the periarticular tissue homogenate (F). Neutrophils with apoptotic morphology were evaluated by morphological examination in cytospin counting at 6 h after PF-04217903 treatment and expressed as percent of neutrophil with apoptotic morphology (G). Apoptosis was biochemically determined 3 h after treatment with PF-04217903 and the median of fluorescence intensity (MFI) of annexin-V on $Ly6G^+$ cells was determined by flow cytometry (H). Representative histogram of annexin-V on $Ly6G^+$ cells (I). Results are shown as the mean ± SEM of five mice in each group, significance was calculated using one-way ANOVA followed by Tukey's test. The specified p-values are shown in the figure.

treatment with zVAD alone did not alter neutrophil recruitment after MSU injection.

In accordance with our in vivo data, PF-04217903-induced human neutrophil apoptosis was abrogated by zVAD-fmk 2 h after LPS/HGF stimulation, as showed by both the percentage (Fig. 7 A) and MFI of annexin-V staining (Fig. 7 C). See supplementary Fig. 5B for gating strategy. Additionally, to confirm the relevance of the HGF/MET pathway suppression by PF-04217903 in the crosstalk between neutrophil survival and inflammation, flow cytometry was carried out to determine the levels of key intracellular proteins that regulate neutrophil fate. Representative dot plots of gating strategy are shown in supplementary Fig. 4B. We observed that suppression of P-MET by PF-04217903 in LPS/HGF-stimulated human neutrophils increased the cleavage of the pro-apoptotic protein caspase-3 (Fig. 7D), while Bcl-xL, an anti-apoptotic protein associated with neutrophil survival, was reduced (Fig. 7E). Representative dot plots and histograms are shown in Fig. 7B and F, respectively.

Collectively, these findings support the idea that the pharmacological inhibition of the HGF/MET pathway by PF-04217903 affects neutrophil survival in vivo and in vitro by inducing caspase-dependent apoptosis to resolve inflammation.

3.7. HGF/MET pathway inhibition increases the ability of macrophages to uptake apoptotic cells

As inhibition of the HGF/MET axis resolved articular inflammation by increasing efferocytosis in the synovial cavity, we further performed an additional approach to investigate the direct impact of the HGF/MET pathway inhibition on the ability of macrophages to uptake apoptotic cells by using an in vivo efferocytosis assay. Thus, mice bearing 90 h peritonitis triggered by zymosan (0.1 mg/cavity) received PF-04217903 (40 mg/kg, via oral gavage) and 6 h later they were injected with the same number of CFSE-labeled apoptotic thymocytes into the peritoneal cavity. Cells were harvested 30 min after the injection of apoptotic thymocytes and efferocytosis was evaluated by flow cytometry and light microscopy (Fig. 8 A). PF-04217903 induced increased efferocytosis rates, as observed by the higher percentage of $F4/80^+CFSE^+$ cells (Fig. 8B, C) or MFI of $CFSE^+$ in macrophages (Fig. 8D, E) and the higher percentage of macrophages that ingested apoptotic thymocytes, as observed in cytospin slide counting (Fig. 8 F, G). Collectively, these findings support the idea that the pharmacological blockage of the HGF/MET pathway ameliorates macrophage ability to optimally execute efferocytosis.

4. Discussion

A critical feature of the inflammation resolution program is the reduction of neutrophil accumulation in inflammatory exudates, which is regulated not only by their trafficking but also by their death and elimination by efferocytosis. In this study, we demonstrated that the HGF/MET pathway is an important axis involved in regulating the inflammatory response and potentially modulates neutrophil survival and the course of neutrophilic inflammation induced by MSU crystals and LPS. Moreover, we demonstrated that pharmacological inhibition of HGF/MET activation initiates pro-resolving programs, increasing neutrophil apoptosis, efferocytosis and AnxA1 expression. We also demonstrated that human neutrophils display an extended lifespan after stimulation with LPS and HGF and that interference with the HGF/MET pathway limited the survival of these cells. Our findings provide a novel neutrophil survival pathway that can be regulated to turn on appropriate tissue resolution programs to reverse neutrophil-dominated inflammatory diseases (summarized in Fig. 9).

MET activation has already been described to regulate the immune response by acting in different immune cell types [39,40], including neutrophils [42]. MET is expressed at low levels in neutrophils under physiological settings but can be upregulated when exposed to distinct inflammatory stimuli, such as LPS, TNF-α, or fMLP [43,70]. There are studies indicating an association of the HGF/MET axis with exacerbated inflammation in several inflammatory conditions, notably rheumatoid arthritis. HGF and MET are expressed in synovial cells and fluid from arthritic patients and are correlated with disease severity and poor outcome [34,71,72]. Serum HGF has been suggested as a biomarker of joint damage severity in patients with rheumatoid arthritis [73]. Of note, P-MET and HGF were overexpressed during MSU-induced gout in mice. Supporting these previous reports, our studies on human neutrophils confirmed that HGF, LPS, or MSU stimulation results in MET phosphorylation. Both in vitro and in vivo MET phosphorylation was efficiently inhibited by PF-04217903. These results indicate that a proinflammatory milieu increases HGF expression, which leads neutrophils to amplify MET phosphorylation.

Blockade of HGF by administration of a competitive antagonist inhibits bone destruction associated with decreased IL-1, IL-6, and TNF-a levels in arthritic mice [74]. Studies also showed that MET activation increased adhesion molecule expression, which rapidly increases neutrophil recruitment during inflammatory processes, and that systemic blockade of MET phosphorylation by PF-04217903 or MET deletion abolished neutrophil trafficking and reduced the proinflammatory environment [38,42,45]. Consistent with these reports, blocking the neutrophilic HGF/MET axis using PF-04217903 treatment reduced articular inflammation in MSU-induced gouty arthritis, as indicated by a reduction in the number of neutrophils and MPO, as well as low levels of CXCL1 and IL-1β in the knee joint. Of interest, the major discovery in our study was that PF-04217903 not only reduces joint inflammation but also modifies the course of inflammation by stimulating the crucial steps of the resolution of the inflammatory response in vivo, including neutrophil apoptosis and efferocytosis, an effect also observed in the LPS-inflamed pleural cavity. Importantly, MET inhibition occurred after neutrophils had migrated to the inflammatory site. These findings indicate that the HGF/MET axis is crucial for determining neutrophil fate in acute inflammatory experimental model settings regardless of stimuli, representing a promising target for the control of inflammatory responses.

Numerous reports in the literature have already shown that neutrophil apoptosis precedes and cooperates with efficient neutrophilic acute inflammation resolution [6,75]. The HGF/MET axis has been reported to provide protection from apoptosis by reducing caspase-3 activity in some cancer cell types [76,77]. Blocking HGF/MET signalling using a competitive inhibitor homologous to HGF can also override prosurvival cues and redirect human fibroblast-like synoviocytes in vitro to apoptosis. Consistently, we demonstrated that MET phosphorylation

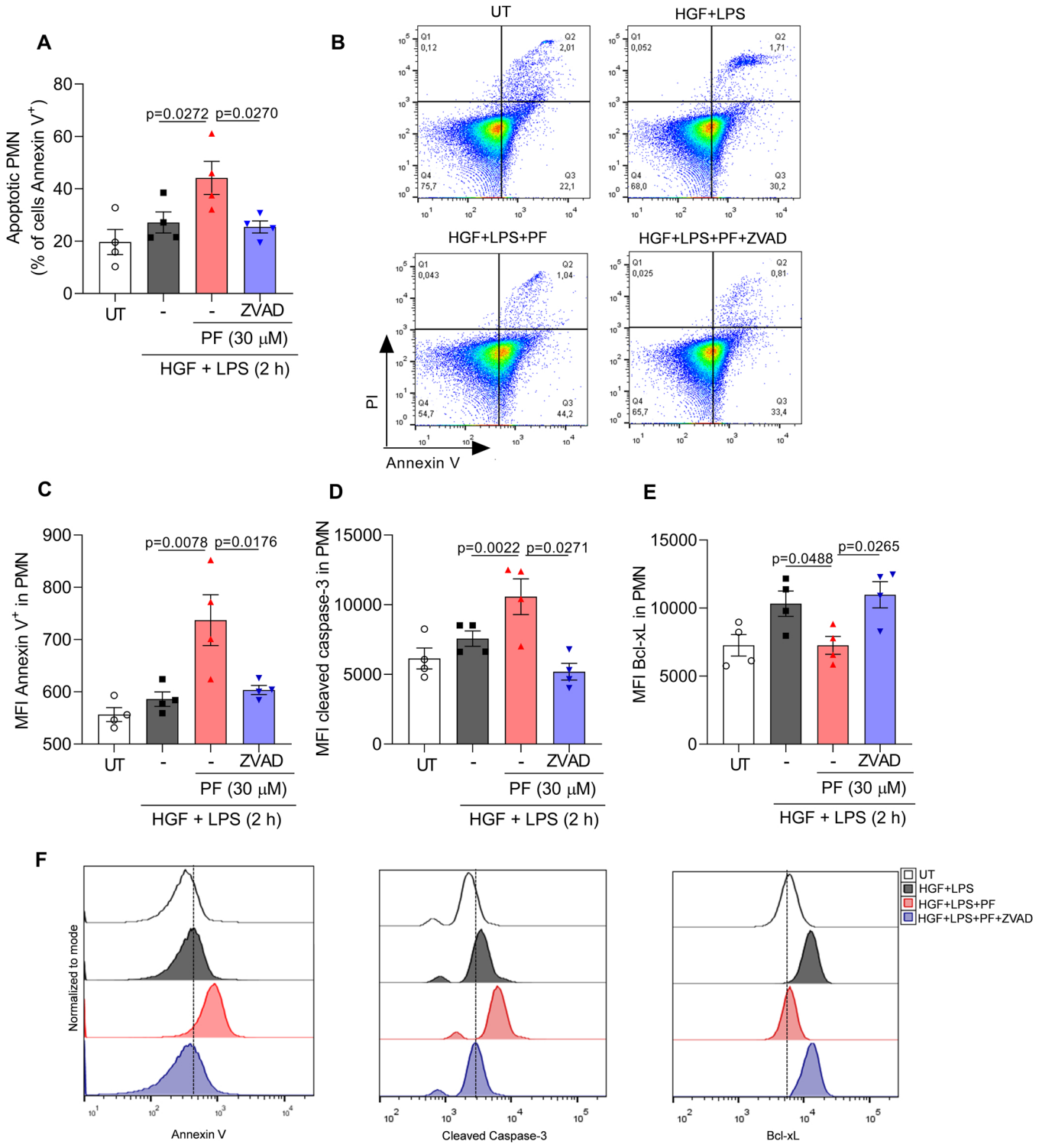

Fig. 7. Inhibition of the HGF/MET pathway on human neutrophil apoptosis and effect of zVAD-fmk. Neutrophils were isolated from the human peripheral blood and pre-treated with zVAD-fmk (15 μM) for 15 min followed by PF-04217903 (30 μM) for 1 h and by further incubation with LPS (1 μg/mL) and HGF (100 ng/mL) for 2 h. Flow cytometry was performed for apoptosis evaluation. The frequency of Annexin-V$^+$ cells (A) and representative dot plots are demonstrated (B). The median of fluorescence intensity (MFI) of annexin-V$^+$ on positive human neutrophil are graphed in (C). Flow cytometry also was used to evaluate MFI of cleaved caspase-3$^+$ (D) and Bcl-xL$^+$ (E). Representative histograms are shown in (F). The experiment is a representative of three independent experiments performed in biological triplicates and is shown as the mean ± SEM, significance was calculated using one-way ANOVA followed by Tukey's test. The specified p-values are shown in the figure.

was associated with prolonged neutrophil survival in vitro and in vivo under an inflammatory setting, and PF-04217903 was able to induce neutrophil apoptosis, with activation of caspase-3 and inhibition of the important prosurvival protein Bcl-xL. More importantly, the blockade of caspases with zVAD-fmk prevented PF-04217903-induced apoptosis and resolution of neutrophilic inflammation. An interesting finding is that the PF-04217903-mediated apoptosis observed in neutrophils was unaltered in mononuclear cells. This is relevant data since mononuclear cells exhibit a crucial role during the resolution process by promoting apoptotic cell clearance and secreting anti-inflammatory and/or

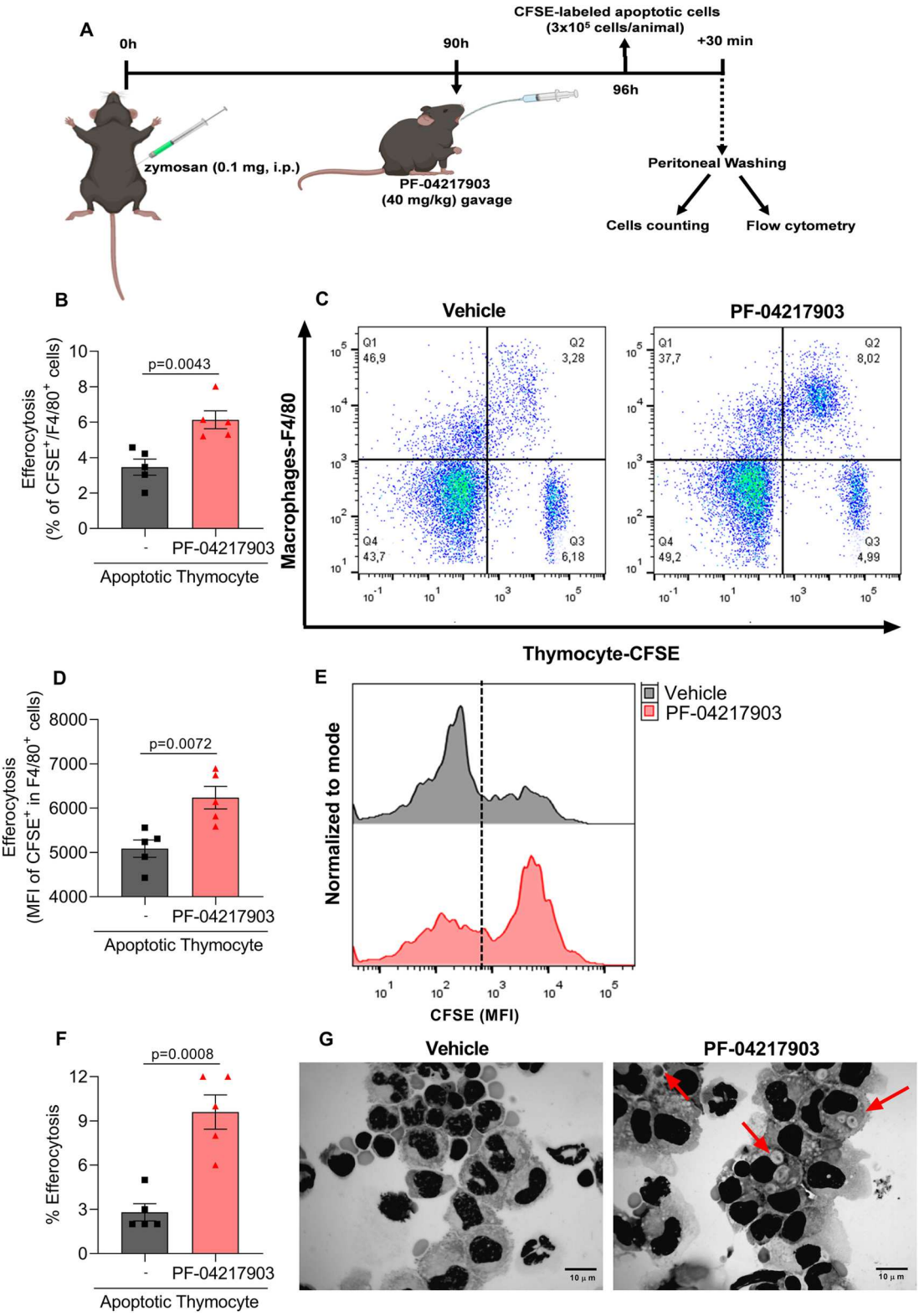

Fig. 8. Inhibition of the HGF/MET pathway and effect on efferocytosis. Mice received an i.p. injection of 0.1 mg of zymosan and 90 h later were treated with PF-04217903 (40 mg/kg) by gavage. Mice received an i.p. injection of 3×10^6 apoptotic thymocytes labeled with fluorescent CFSE 6 h after treatment with PF-04217903. The cells from the peritoneal cavity were collected 30 min later (A). Efferocytosis was assessed by flow cytometry. The frequency of double-positive cells for CFSE and F4/80 (B) and representative dot plots are demonstrated (C). The median of fluorescence intensity (MFI) of CFSE-labeled thymocyte on positive F4/80 cells (D) and representative histograms are demonstrated (E). Efferocytosis was also evaluated by cytospin counting (F) and images of apoptotic thymocytes ingested by macrophages (arrows) are shown (G). Magnification x100. Results are shown as the mean ± SEM of n = 5 in each group. Significance was calculated using one-way ANOVA followed by Tukey's test. The specified p-values are shown in the figure.

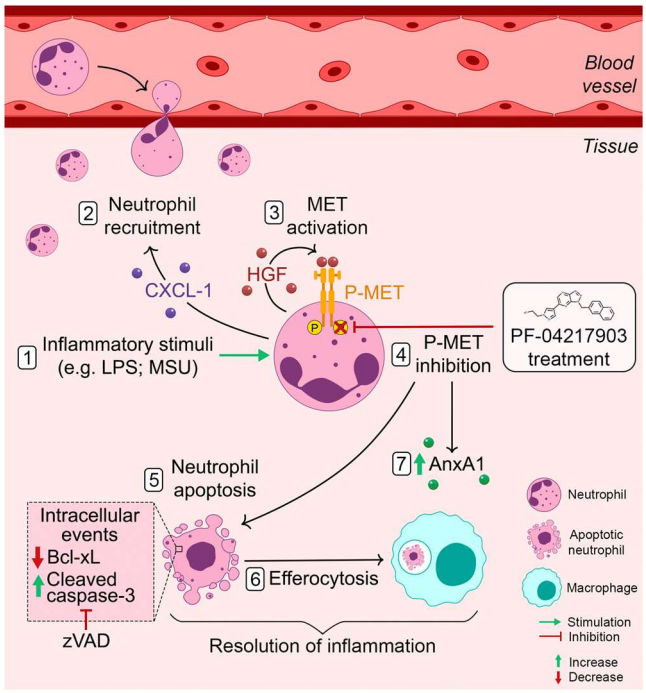

Fig. 9. Schematic representation of the effect of the HGF-MET pathway blocking by PF-04217903 on the resolution of neutrophilic inflammation. (1,2) In inflammatory sites, recruited neutrophils induced by LPS and MSU stimuli result in HGF overexpression and, (3) consequently, MET phosphorylation in a paracrine- and autocrine-dependent manner. (4) Blocking MET activation (and consequently phosphorylation) by PF-04217903 accelerate the neutrophilic inflammation resolution by inducing (5) neutrophil apoptosis, with activation of caspase-3 and inhibition of the prosurvival protein BclxL, which is abrogated by zVAD-fmk treatment, a broad-spectrum caspase inhibitor. (6) PF-04217903 enhances macrophage ability to optimally remove apoptotic cells through efferocytosis. (7) Importantly, PF-04217903-induced inflammation resolution is associated with enhancement of Annexin A1 expression on neutrophil and macrophages, thereby, helping to successful tissue resolution.

pro-resolutive mediators [78]. Collectively, we provide strong evidence that the HGF/MET pathway represents a powerful prosurvival signalling pathway in neutrophils, and a therapeutic strategy targeting this axis may interfere with the lifespan of these cells, facilitating neutrophil-dominated inflammation resolution via apoptosis induction.

Previous studies have shown that macrophages stimulated with HGF, LPS, and TNF exhibit high levels of MET expression and phosphorylation [79,80]. Interestingly, the HGF/MET pathway seems to play a dual role in macrophage functions [39]. The HGF/MET pathway can directly contribute to the maintenance of a proinflammatory profile correlated with disease severity in experimental autoimmune encephalomyelitis [79] and ischaemic retinopathy [81]. However, it was also described that HGF/MET promotes the transition of macrophages to an anti-inflammatory profile favouring muscle repair [82,83]. Anti-inflammatory macrophages exhibit a high capacity to remove apoptotic neutrophils from the inflamed area (efferocytosis), a key pro-resolving function for the efficient resolution of inflammation and return to homeostasis [18,84]. The key point revealed here, which is consistent with these previous reports, is that the blockage of the HGF/MET pathway by PF-04217903 enhances the ability of macrophages to optimally execute efferocytosis to assure timely resolution of inflammation. Although our study did not directly focus on the influence of the HGF/MET pathway on macrophages, we can suggest that in the context of efferocytosis, blocking MET phosphorylation may result in the production of efferocytosis-related immunoregulatory molecules or promote the phenotypic alteration of macrophages toward an anti-inflammatory and restorative profile, which has a higher efferocytic capacity and proresolving actions. However, further investigation of the effect of HGF/MET axis blocking by PF-04217903 on macrophages is needed in the future to better understand the functionality of the HGF/MET axis in the intimate partnership between macrophages and the resolution of inflammation.

Joint pain is a marked debilitating symptom in gouty patients that is associated to tissue loss of function, which is closed related to excessive neutrophil activity It is known that loss of function is closely associated with severe joint pain, which is a marked debilitating symptom in arthritic patients, and this is closely related to excessive neutrophil activity [85]. Both intense CXCL1-mediated neutrophil influx and the production of hyperalgesic mediators, such as IL-1β, in the synovial cavity are required for hypernociception generation [55,67]. In agreement with these previous studies, we demonstrated that treatment of arthritic mice with PF-04217903 reduced histopathological score and pain by reducing the secretion of CXCL1 and IL-1β in the periarticular tissue. Altogether, these data reinforce that the HGF/MET axis may be involved in maintaining articular neutrophilic inflammatory responses, and inhibition of this pathway by PF-04217903 could be a possible pro-resolving strategy to prevent or reverse neutrophil-mediated tissue damage.

Mechanistically, PF-0417903 mediated protective effects were associated to an increased expression of the proresolving protein AnxA1 in both macrophages and neutrophils. These findings are in line with the known expression of AnxA1 by a variety of immune cells, and the ability to mediate, among different actions, the apoptosis and efferocytosis of granulocytes and reduction of the overall production of inflammatory mediators in the context of different diseases [68,69]. Of note, AnxA1 was shown to be crucial for resolution of MSU-induced inflammation in the joint leading to a better outcome from disease [86]. Therefore, here, we describe a novel molecular mechanism for the resolution of inflammation induced by HGF/MET blockage during joint inflammation.

In summary, the current study identified the HGF/MET axis as a powerful modulator of neutrophil fate in the inflammatory site. HGF provides a pro-survival signal for neutrophils in vitro and blocking MET by PF-04217903 notably induced the activation of a pro-resolution program characterized by reduced neutrophil lifespan and enhanced efferocytosis (summarized in Fig. 9). Altogether, the latter actions were accompanied by successful tissue repair and decreased joint damage and pain. Therefore, a therapeutic strategy targeting the HGF/MET axis could be fundamental to disrupting the consolidated crosstalk between neutrophil survival and the inflammatory response and could be an effective pharmacological approach to control neutrophil-mediated inflammatory diseases.

Funding

This work was supported by grants from National Institute of Science and Technology in Dengue and Host-Microbial Interactions, a program grant from Conselho Nacional de Desenvolvimento Científico e Tecnológico (CNPq), Fundação de Amparo à Pesquisa do Estado de Minas Gerais (FAPEMIG, Brazil), Coordenação de Aperfeiçoamento de Pessoal de Nível Superior (CAPES, Brazil) Financial Code 001. This work also was supported by Ministério da Ciência, Tecnologia e Inovações (MCTI)/CNPQ/CAPES/FAPS (Fundações de Amparo à Pesquisa), grant number 16/2014-Programa dos Institutos Nacionais de Ciência e Tecnologia (INCT) 465425/2014-3; L.P, F.A.A, F.M.S, M.T.T. and V.P. receive scholarships from CNPq.

CRediT authorship contribution statement

F.B.F., J.P.V., V.P. analyzed data and wrote the paper. F.B.F., J.D., V. A.B., D.G.M., D.O.F., A.C.P.M.S., C.M.Q-J., F.M.S. performed the experiments and analyzed data. L.P.S., F.A.A., M.M.T. provided expertise and improvements in the issue and helped with paper discussion. V.P designed research. F.B.F and J.D. have contributed equally to the

technical and scientific aspects of the work. All authors have read and agreed to the published version of the manuscript.

Conflict of interest

The authors have declared that no conflict of interest exists.

Data Availability

Data will be made available on request.

Acknowledgments

We would like to thank Frankcineia Assis, Rosemeire Oliveira, Ilma Marçal, Alysson Cramer and Hermes Oliveira for their technical assistance.

Appendix A. Supporting information

Supplementary data associated with this article can be found in the online version at doi:10.1016/j.phrs.2022.106640.

References

[1] R. Medzhitov, Inflammation 2010: new adventures of an old flame, Cell 140 (2010) 771–776, https://doi.org/10.1016/j.cell.2010.03.006.
[2] R. Medzhitov, The spectrum of inflammatory responses, Sci. (80-.) 374 (2021) 1070–1075, https://doi.org/10.1126/SCIENCE.ABI5200.
[3] M.L. Meizlish, R.A. Franklin, X. Zhou, R. Medzhitov, Tissue homeostasis and inflammation, Annu. Rev. Immunol. 39 (2021) 557–581, https://doi.org/10.1146/annurev-immunol-061020-053734.
[4] E. Kolaczkowska, P. Kubes, Neutrophil recruitment and function in health and inflammation, Nat. Rev. Immunol. 13 (2013) 159–175, https://doi.org/10.1038/nri3399.
[5] W.M. Nauseef, N. Borregaard, Neutrophils at work, Nat. Immunol. 15 (2014) 602–611, https://doi.org/10.1038/ni.2921.
[6] D. El Kebir, J.G. Filep, Targeting neutrophil apoptosis for enhancing the resolution of inflammation, Cells 2 (2013) 330–348, https://doi.org/10.3390/cells2020330.
[7] A. Hidalgo, M. Casanova-Acebes, Dimensions of neutrophil life and fate, Semin. Immunol. (2021), 101506, https://doi.org/10.1016/j.smim.2021.101506.
[8] C. Nathan, Nonresolving inflammation redux, Immunity 55 (2022) 592–605, https://doi.org/10.1016/j.immuni.2022.03.016.
[9] D. Furman, J. Campisi, E. Verdin, P. Carrera-Bastos, S. Targ, C. Franceschi, L. Ferrucci, D.W. Gilroy, A. Fasano, G.W. Miller, A.H. Miller, A. Mantovani, C. M. Weyand, N. Barzilai, J.J. Goronzy, T.A. Rando, R.B. Effros, A. Lucia, N. Kleinstreuer, G.M. Slavich, Chronic inflammation in the etiology of disease across the life span, Nat. Med. 25 (2019) 1822–1832, https://doi.org/10.1038/s41591-019-0675-0.
[10] T.H. Zaninelli, V. Fattori, W.A. Verri, Harnessing inflammation resolution in arthritis: current understanding of specialized pro-resolving lipid mediators' contribution to arthritis physiopathology and future perspectives, Front. Physiol. 12 (2021) 1–16, https://doi.org/10.3389/fphys.2021.729134.
[11] M. Bäck, A. Yurdagul, I. Tabas, K. Öörni, P.T. Kovanen, Inflammation and its resolution in atherosclerosis: mediators and therapeutic opportunities, Nat. Rev. Cardiol. 16 (2019) 389–406, https://doi.org/10.1038/s41569-019-0169-2.
[12] G.S. Hotamisligil, Inflammation, metaflammation and immunometabolic disorders, Nature 542 (2017) 177–185, https://doi.org/10.1038/nature21363.
[13] J.F. Gregório, M. da, G. Rodrigues-Machado, R.A.S. Santos, I.A. Carvalho-Ribeiro, O.M. Nunes, I.F.A. Oliveira, A.V. de, O. Vasconcellos, M.J. Campagnole-Santos, G. S. Magalhães, Asthma: role of the angiotensin-(1-7)/Mas (MAS1) pathway in pathophysiology and therapy, Br. J. Pharmacol. (2021), https://doi.org/10.1111/bph.15619.
[14] D. Panigrahy, M.M. Gilligan, C.N. Serhan, K. Kashfi, Resolution of inflammation: an organizing principle in biology and medicine, Pharmacol. Ther. 227 (2021), https://doi.org/10.1016/j.pharmthera.2021.107879.
[15] A. Fishbein, B.D. Hammock, C.N. Serhan, D. Panigrahy, Carcinogenesis: failure of resolution of inflammation, Pharmacol. Ther. 218 (2021), https://doi.org/10.1016/j.pharmthera.2020.107670.
[16] I.K.H. Poon, C.D. Lucas, A.G. Rossi, K.S. Ravichandran, Apoptotic cell clearance: basic biology and therapeutic potential, Nat. Rev. Immunol. 14 (2014) 166–180, https://doi.org/10.1038/nri3607.
[17] M.C. Greenlee-Wacker, Clearance of apoptotic neutrophils and resolution of inflammation, Immunol. Rev. 273 (2016) 357–370, https://doi.org/10.1111/imr.12453.
[18] A.C. Doran, A. Yurdagul, I. Tabas, Efferocytosis in health and disease, Nat. Rev. Immunol. 20 (2020) 254–267, https://doi.org/10.1038/s41577-019-0240-6.
[19] M.A. Sugimoto, J.P. Vago, M. Perretti, M.M. Teixeira, Mediators of the Resolution of the Inflammatory Response, Trends Immunol. 40 (2019) 212–227, https://doi.org/10.1016/j.it.2019.01.007.
[20] B.V.S. Valiate, C.M. Queiroz-Junior, F. Levi-Schaffer, I. Galvão, M.M. Teixeira, CD300a contributes to the resolution of articular inflammation triggered by MSU crystals by controlling neutrophil apoptosis, Immunology 164 (2021) 305–317, https://doi.org/10.1111/imm.13371.
[21] I. Galvão, E.M. Melo, V.L.S. de Oliveira, J.P. Vago, C. Queiroz-Junior, M. de Gaetano, E. Brennan, K. Gahan, P.J. Guiry, C. Godson, M.M. Teixeira, Therapeutic potential of the FPR2/ALX agonist AT-01-KG in the resolution of articular inflammation, Pharmacol. Res. 165 (2021), https://doi.org/10.1016/j.phrs.2021.105445.
[22] G.S. Magalhaes, L.C. Barroso, A.C. Reis, M.G. Rodrigues-Machado, J.F. Gregório, D. Motta-Santos, A.C. Oliveira, D.A. Perez, L.S. Barcelos, M.M. Teixeira, R.A. S. Santos, V. Pinho, M.J. Campagnole-Santos, Angiotensin-(1-7) promotes resolution of eosinophilic inflammation in an experimental model of asthma, Front. Immunol. 9 (2018) 1–10, https://doi.org/10.3389/fimmu.2018.00058.
[23] A. Yurdagul, M. Subramanian, X. Wang, S.B. Crown, O.R. Ilkayeva, L. Darville, G. K. Kolluru, C.C. Rymond, B.D. Gerlach, Z. Zheng, G. Kuriakose, C.G. Kevil, J. M. Koomen, J.L. Cleveland, D.M. Muoio, I. Tabas, Macrophage metabolism of apoptotic cell-derived arginine promotes continual efferocytosis and resolution of injury, e10, Cell Metab. 31 (2020) 518–533, https://doi.org/10.1016/j.cmet.2020.01.001.
[24] J. Zhao, W. Zhang, T. Wu, H. Wang, J. Mao, J. Liu, Z. Zhou, X. Lin, H. Yan, Q. Wang, Efferocytosis in the central nervous system, Front. Cell Dev. Biol. 9 (2021) 1–14, https://doi.org/10.3389/fcell.2021.773344.
[25] V. Finisguerra, H. Prenen, M. Mazzone, Preclinical and clinical evaluation of MET functions in cancer cells and in the tumor stroma, Oncogene 35 (2016) 5457–5467, https://doi.org/10.1038/onc.2016.36.
[26] C.A. Bradley, M. Salto-Tellez, P. Laurent-Puig, A. Bardelli, C. Rolfo, J. Tabernero, H.A. Khawaja, M. Lawler, P.G. Johnston, S. Van Schaeybroeck, Targeting c-MET in gastrointestinal tumours: rationale, opportunities and challenges, Nat. Rev. Clin. Oncol. 14 (2017) 562–576, https://doi.org/10.1038/nrclinonc.2017.40.
[27] D.G.F. Al-U'datt, B.A.A. Al-Husein, G.R. Qasaimeh, A mini-review of c-Met as a potential therapeutic target in melanoma, Biomed. Pharmacother. 88 (2017) 194–202, https://doi.org/10.1016/j.biopha.2017.01.045.
[28] E. Uchikawa, Z. Chen, G.Y. Xiao, X. Zhang, X. chen Bai, Structural basis of the activation of c-MET receptor, Nat. Commun. 12 (2021), https://doi.org/10.1038/s41467-021-24367-3.
[29] J.P. Koch, D.M. Aebersold, Y. Zimmer, M. Medová, MET targeting: time for a rematch, Oncogene 39 (2020) 2845–2862, https://doi.org/10.1038/s41388-020-1193-8.
[30] J. Fu, X. Su, Z. Li, L. Deng, X. Liu, X. Feng, J. Peng, HGF/c-MET pathway in cancer: from molecular characterization to clinical evidence, Oncogene 40 (2021) 4625–4651, https://doi.org/10.1038/s41388-021-01863-w.
[31] P.M. Comoglio, L. Trusolino, C. Boccaccio, Known and novel roles of the MET oncogene in cancer: a coherent approach to targeted therapy, Nat. Rev. Cancer 18 (2018) 341–358, https://doi.org/10.1038/s41568-018-0002-y.
[32] I. Yeh, T. Botton, E. Talevich, A.H. Shain, A.J. Sparatta, A. De La Fouchardiere, T. W. Mully, J.P. North, M.C. Garrido, A. Gagnon, S.S. Vemula, T.H. McCalmont, P. E. Leboit, B.C. Bastian, Activating MET kinase rearrangements in melanoma and Spitz tumours, Nat. Commun. 6 (2015) 1–9, https://doi.org/10.1038/ncomms8174.
[33] R. Guo, J. Luo, J. Chang, N. Rekhtman, M. Arcila, A. Drilon, MET-dependent solid tumours — molecular diagnosis and targeted therapy, Nat. Rev. Clin. Oncol. 17 (2020) 569–587, https://doi.org/10.1038/s41571-020-0377-z.
[34] M. Hosonuma, N. Sakai, H. Furuya, Y. Kurotaki, Y. Sato, K. Handa, Y. Dodo, K. Ishikawa, Y. Tsubokura, T. Negishi-Koga, M. Tsuji, T. Kasama, Y. Kiuchi, M. Takami, T. Isozaki, Inhibition of hepatocyte growth factor/c-Met signalling abrogates joint destruction by suppressing monocyte migration in rheumatoid arthritis, Rheumatol. (U. Kingd.) 60 (2021) 408–419, https://doi.org/10.1093/rheumatology/keaa310.
[35] E. Abed, B. Bouvard, X. Martineau, J.Y. Jouzeau, P. Reboul, D. Lajeunesse, Elevated hepatocyte growth factor levels in osteoarthritis osteoblasts contribute to their altered response to bone morphogenetic protein-2 and reduced mineralization capacity, Bone 75 (2015) 111–119, https://doi.org/10.1016/j.bone.2015.02.001.
[36] M. Benkhoucha, N.L. Tran, G. Breville, I. Senoner, P.F. Bradfield, T. Papayannopoulou, D. Merkler, T. Korn, P.H. Lalive, CD4+c-Met+Itgα4+ T cell subset promotes murine neuroinflammation, J. Neuroinflam. (2022) 1–19, https://doi.org/10.1186/s12974-022-02461-7.
[37] J. Guo, S. Wang, H. Xia, D. Shi, Y. Chen, S. Zheng, Y. Chen, H. Gao, F. Guo, Z. Ji, C. Huang, R. Luo, Y. Zhang, J. Zuo, Y. Chen, Y. Xu, J. Xia, C. Zhu, X. Xu, Y. Qiu, J. Sheng, K. Xu, L. Li, Cytokine signature associated with disease severity in COVID-19, Front. Immunol. 12 (2021) 1–10, https://doi.org/10.3389/fimmu.2021.681516.
[38] M. Stakenborg, B. Verstockt, E. Meroni, G. Goverse, V. De Simone, S. Verstockt, M. Di Matteo, P. Czarnewski, E.J. Villablanca, M. Ferrante, G.E. Boeckxstaens, M. Mazzone, S. Vermeire, G. Matteoli, Neutrophilic HGF-MET signalling exacerbates intestinal inflammation, J. Crohns. Colitis 14 (2020) 1748–1758, https://doi.org/10.1093/ecco-jcc/jjaa121.
[39] S. Ilangumaran, A. Villalobos-Hernandez, D. Bobbala, S. Ramanathan, The hepatocyte growth factor (HGF)-MET receptor tyrosine kinase signaling pathway: diverse roles in modulating immune cell functions, Cytokine 82 (2016) 125–139, https://doi.org/10.1016/j.cyto.2015.12.013.
[40] N. Molnarfi, M. Benkhoucha, H. Funakoshi, T. Nakamura, P.H. Lalive, Hepatocyte growth factor: a regulator of inflammation and autoimmunity, Autoimmun. Rev. 14 (2015) 293–303, https://doi.org/10.1016/j.autrev.2014.11.013.
[41] M. Benkhoucha, N.L. Tran, G. Breville, I. Senoner, C. Jandus, P. Lalive, c-Met enforces proin fl ammatory and migratory features of human activated CD4 + T

cells, Cell. Mol. Immunol. (2021) 4–6, https://doi.org/10.1038/s41423-021-00721-9.
[42] V. Finisguerra, G. Di Conza, M. Di Matteo, J. Serneels, A.A.R. Thompson, E. Wauters, S. Walmsley, H. Prenen, Z. Granot, A. Casazza, M. Mazzone, Europe PMC funders group Europe PMC funders author manuscripts MET is required for the recruitment of anti-tumoural neutrophils, Nature 522 (2015) 349–353, https://doi.org/10.1038/nature14407.MET.
[43] M. McCourt, J.H. Wang, S. Sookhai, H.P. Redmond, Activated human neutrophils release hepatocyte growth factor/scatter factor, Eur. J. Surg. Oncol. 27 (2001) 396–403, https://doi.org/10.1053/ejso.2001.1133.
[44] A. Grenier, S. Chollet-Martin, B. Crestani, C. Delarche, J. El Benna, A. Boutten, V. Andrieu, G. Durand, M.A. Gougerot-Pocidalo, M. Aubier, M. Dehoux, Presence of a mobilizable intracellular pool of hepatocyte growth factor in human polymorphonuclear neutrophils, Blood 99 (2002) 2997–3004, https://doi.org/10.1182/blood.V99.8.2997.
[45] N. Glodde, T. Bald, D. van den Boorn-Konijnenberg, K. Nakamura, J.S. O'Donnell, S. Szczepanski, M. Brandes, S. Eickhoff, I. Das, N. Shridhar, D. Hinze, M. Rogava, T. C. van der Sluis, J.J. Ruotsalainen, E. Gaffal, J. Landsberg, K.U. Ludwig, C. Wilhelm, M. Riek-Burchardt, A.J. Müller, C. Gebhardt, R.A. Scolyer, G.V. Long, V. Janzen, M.W.L. Teng, W. Kastenmüller, M. Mazzone, M.J. Smyth, T. Tüting, M. Hölzel, Reactive neutrophil responses dependent on the receptor tyrosine kinase c-MET limit cancer immunotherapy, e9, Immunity 47 (2017) 789–802, https://doi.org/10.1016/j.immuni.2017.09.012.
[46] T. Underiner, T. Herbertz, S. Miknyoczki, Discovery of small molecule c-met inhibitors: evolution and profiles of clinical candidates, Anticancer. Agents Med. Chem. 10 (2012) 7–27, https://doi.org/10.2174/1871520611009010007.
[47] C. Chu, Z. Rao, Q. Pan, W. Zhu, An updated patent review of small-molecule c-Met kinase inhibitors (2018-present, Expert Opin. Ther. Pat. 32 (2022) 279–298, https://doi.org/10.1080/13543776.2022.2008356.
[48] J.J. Cui, M. McTigue, M. Nambu, M. Tran-Dubé, M. Pairish, H. Shen, L. Jia, H. Cheng, J. Hoffman, P. Le, M. Jalaie, G.H. Goetz, K. Ryan, N. Grodsky, Y.L. Deng, M. Parker, S. Timofeevski, B.W. Murray, S. Yamazaki, S. Aguirre, Q. Li, H. Zou, J. Christensen, Discovery of a novel class of exquisitely selective mesenchymal-epithelial transition factor (c-MET) protein kinase inhibitors and identification of the clinical candidate 2-(4-(1-(Quinolin-6-ylmethyl)-1H -[1,2,3]triazolo[4,5- b] pyrazin-6-yl)-1H -pyraz, J. Med. Chem. 55 (2012) 8091–8109, https://doi.org/10.1021/jm300967g.
[49] H.Y. Zou, Q. Li, J.H. Lee, M.E. Arango, K. Burgess, M. Qiu, L.D. Engstrom, S. Yamazaki, M. Parker, S. Timofeevski, J.J. Cui, M. McTigue, G. Los, S.L. Bender, T. Smeal, J.G. Christensen, Sensitivity of selected human tumor models to PF-04217903, a novel selective c-Met kinase inhibitor, Mol. Cancer Ther. 11 (2012) 1036–1047, https://doi.org/10.1158/1535-7163.MCT-11-0839.
[50] B. Sennino, T. Ishiguro-Oonuma, Y. Wei, R.M. Naylor, C.W. Williamson, V. Bhagwandin, S.P. Tabruyn, W.K. You, H.A. Chapman, J.G. Christensen, D. T. Aftab, D.M. McDonald, Suppression of tumor invasion and metastasis by concurrent inhibition of c-Met and VEGF signaling in pancreatic neuroendocrine tumors, Cancer Disco 2 (2012) 270–287, https://doi.org/10.1158/2159-8290.CD-11-0240.
[51] Y. Wu, Q. Fan, F. Zeng, J. Zhu, J. Chen, D. Fan, X. Li, W. Duan, Q. Guo, Z. Cao, K. Briley-Saebo, C. Li, X. Tao, Peptide-functionalized nanoinhibitor restrains brain tumor growth by abrogating mesenchymal-epithelial Transition Factor (MET) signaling, Nano Lett. 18 (2018) 5488–5498, https://doi.org/10.1021/acs.nanolett.8b01879.
[52] H.S. Cheng, C. Marvalim, P. Zhu, C.L. Daniel Law, Z.Y. Jeremy Low, Y.K. Chong, B. T. Ang, C. Tang, N.S. Tan, Kinomic profile in patient-derived glioma cells during hypoxia reveals c-MET-PI3K dependency for adaptation, Theranostics 11 (2021) 5127–5142, https://doi.org/10.7150/thno.54741.
[53] J.R. Diamond, R. Salgia, M. Varella-Garcia, R. Kanteti, P.M. LoRusso, J.W. Clark, L. G. Xu, K. Wilner, S.G. Eckhardt, K.A. Ching, M.E. Lira, E.F.P.M. Schoenmakers, J. G. Christensen, D.R. Camidge, Initial clinical sensitivity and acquired resistance to MET inhibition in MET-mutated papillary renal cell carcinoma, J. Clin. Oncol. 31 (2013) 254–258, https://doi.org/10.1200/JCO.2012.46.4289.
[54] J.P. Vago, C.R.C. Nogueira, L.P. Tavares, F.M. Soriani, F. Lopes, R.C. Russo, V. Pinho, M.M. Teixeira, L.P. Sousa, Annexin A1 modulates natural and glucocorticoid-induced resolution of inflammation by enhancing neutrophil apoptosis, J. Leukoc. Biol. 92 (2012) 249–258, https://doi.org/10.1189/jlb.0112008.
[55] F.A. Amaral, V.V. Costa, L.D. Tavares, D. Sachs, F.M. Coelho, C.T. Fagundes, F. M. Soriani, T.N. Silveira, L.D. Cunha, D.S. Zamboni, V. Quesniaux, R.S. Peres, T. M. Cunha, F.Q. Cunha, B. Ryffel, D.G. Souza, M.M. Teixeira, NLRP3 inflammasome-mediated neutrophil recruitment and hypernociception depend on leukotriene B4 in a murine model of gout, Arthritis Rheum. 64 (2012) 474–484, https://doi.org/10.1002/art.33355.
[56] F.B. Felix, J.P. Vago, D. de, O. Fernandes, D.G. Martins, I.Z. Moreira, W. A. Gonçalves, W.C. Costa, J.M.D. Araújo, C.M. Queiroz-Junior, G.H. Campolina-Silva, F.M. Soriani, L.P. Sousa, R. Grespan, M.M. Teixeira, V. Pinho, Biochanin A regulates key steps of inflammation resolution in a model of antigen-induced arthritis via GPR30/PKA-dependent mechanism, Front. Pharmacol. 12 (2021) 1–17, https://doi.org/10.3389/fphar.2021.662308.
[57] I. Galvão, C.M. Queiroz-Junior, V.L.S. De Oliveira, V. Pinho, E. Hirsch, M. M. Teixeira, The inhibition of phosphoinositide-3 kinases induce resolution of inflammation in a gout model, Front. Pharmacol. 9 (2019) 1–10, https://doi.org/10.3389/fphar.2018.01505.
[58] W.A. Gonçalves, B.M. Rezende, M.P.E. de Oliveira, L.S. Ribeiro, V. Fattori, W.N. da Silva, P.H.D.M. Prazeres, C.M. Queiroz-Junior, K.T. de, O. Santana, W.C. Costa, V. A. Beltrami, V.V. Costa, A. Birbrair, W.A. Verri, F. Lopes, T.M. Cunha, M. M. Teixeira, F.A. Amaral, V. Pinho, Sensory ganglia-specific TNF expression is associated with persistent nociception after resolution of inflammation, Front. Immunol. 10 (2020) 1–14, https://doi.org/10.3389/fimmu.2019.03120.
[59] C.M. Queiroz-Junior, M.F.M. Madeira, F.M. Coelho, V.V. Costa, R.L.C. Bessoni, L. F. da, C. Sousa, G.P. Garlet, D. da, G. de Souza, M.M. Teixeira, T.A. da Silva, Experimental arthritis triggers periodontal disease in mice: involvement of TNF-α and the oral microbiota, J. Immunol. 187 (2011) 3821–3830, https://doi.org/10.4049/jimmunol.1101195.
[60] I. Galvão, R.M. Athayde, D.A. Perez, A.C. Reis, L. Rezende, V.L.S. de Oliveira, B. M. Rezende, W.A. Gonçalves, L.P. Sousa, M.M. Teixeira, V. Pinho, ROCK inhibition drives resolution of acute inflammation by enhancing neutrophil apoptosis, Cells 8 (2019) 1–21, https://doi.org/10.3390/cells8090964.
[61] D.A. Perez, I. Galvão, R.M. Athayde, B.M. Rezende, J.P. Vago, J.D. Silva, A.C. Reis, L.S. Ribeiro, J.H.S. Gomes, R.M. Pádua, F.C. Braga, L.P. Sousa, M.M. Teixeira, V. Pinho, Inhibition of the sphingosine-1-phosphate pathway promotes the resolution of neutrophilic inflammation, Eur. J. Immunol. 49 (2019) 1038–1051, https://doi.org/10.1002/eji.201848049.
[62] Y. Zhen, W.H. Shao, Experimental analysis of apoptotic thymocyte engulfment by macrophages, J. Vis. Exp. (2019) 1–6, https://doi.org/10.3791/59731.
[63] I. Zaidan, I. Galvão, L.P. Sousa, Angiotensin- (1–7)/ MasR axis promotes migration of monocytes / macrophages with a regulatory phenotype to perform phagocytosis and efferocytosis, (2021).
[64] Graziele L. Negreiros-Lima, K.M. Lima, V. Pinho, M.M. Teixeira, M.A. Sugimoto, P. Sousa, Cyclic AMP regulates key features of macrophages, Cells (2020).
[65] M.J. Curtis, S. Alexander, G. Cirino, J.R. Docherty, C.H. George, M.A. Giembycz, D. Hoyer, P.A. Insel, A.A. Izzo, Y. Ji, D.J. MacEwan, C.G. Sobey, S.C. Stanford, M. M. Teixeira, S. Wonnacott, A. Ahluwalia, Experimental design and analysis and their reporting II: updated and simplified guidance for authors and peer reviewers, Br. J. Pharmacol. 175 (2018) 987–993, https://doi.org/10.1111/bph.14153.
[66] K.M. Lima, J.P. Vago, T.R. Caux, G.L. Negreiros-Lima, M.A. Sugimoto, L.P. Tavares, R.G. Arribada, A.A.F. Carmo, I. Galvão, B.R.C. Costa, F.M. Soriani, V. Pinho, E. Solito, M. Perretti, M.M. Teixeira, L.P. Sousa, The resolution of acute inflammation induced by cyclic AMP is dependent on Annexin A1, J. Biol. Chem. 292 (2017) 13758–13773, https://doi.org/10.1074/jbc.M117.800391.
[67] D. Sachs, F.M. Coelho, V.V. Costa, F. Lopes, V. Pinho, F.A. Amaral, T.A. Silva, A. L. Teixeira, D.G. Souza, M.M. Teixeira, Cooperative role of tumour necrosis factor-α, interleukin-1β and neutrophils in a novel behavioural model that concomitantly demonstrates articular inflammation and hypernociception in mice, Br. J. Pharm. 162 (2011) 72–83, https://doi.org/10.1111/j.1476-5381.2010.00895.x.
[68] M.A. Sugimoto, J.P. Vago, M.M. Teixeira, L.P. Sousa, Annexin A1 and the resolution of inflammation: modulation of neutrophil recruitment, apoptosis, and clearance, J. Immunol. Res. 2016 (2016), https://doi.org/10.1155/2016/8239258.
[69] M. Perretti, F. D'Acquisto, Annexin A1 and glucocorticoids as effectors of the resolution of inflammation, Nat. Rev. Immunol. 9 (2009) 62–70, https://doi.org/10.1038/nri2470.
[70] M. Wislez, N. Rabbe, J. Marchal, B. Milleron, B. Crestani, C. Mayaud, M. Antoine, P. Soler, J. Cadranel, Hepatocyte growth factor production by neutrophils infiltrating bronchioloalveolar subtype pulmonary adenocarcinoma: Role in tumor progression and death, Cancer Res 63 (2003) 1405–1412.
[71] M. Nagashima, J. Hasegawa, K. Kato, J. Yamazaki, K. Nishigai, T. Ishiwata, G. Asano, S. Yoshino, Hepatocyte Growth Factor (HGF), HGF activator, and c-Met in synovial tissues in rheumatoid arthritis and osteoarthritis, J. Rheumatol. 28 (2001) 1772–1778.
[72] S. Shibasaki, S. Tsunemi, S. Kitano, M. Sekiguchi, H. Sano, T. Iwasaki, Differential regulation of c-Met signaling pathways for synovial cell function, Springerplus 3 (2014) 1–7, https://doi.org/10.1186/2193-1801-3-554.
[73] B. Grandaunet, S.W. Syversen, M. Hoff, A. Sundan, G. Haugeberg, D. Van Der Heijde, T.K. Kvien, T. Standal, Association between high plasma levels of hepatocyte growth factor and progression of radiographic damage in the joints of patients with rheumatoid arthritis, Arthritis Rheum. 63 (2011) 662–669, https://doi.org/10.1002/art.30163.
[74] S. Tsunemi, T. Iwasaki, S. Kitano, K. Matsumoto, M. Takagi-Kimura, S. Kubo, T. Tamaoki, H. Sano, Molecular targeting of hepatocyte growth factor by an antagonist, NK4, in the treatment of rheumatoid arthritis, Arthritis Res. Ther. 15 (2013) R75, https://doi.org/10.1186/ar4252.
[75] J.G. Filep, Targeting neutrophils for promoting the resolution of inflammation, Front. Immunol. 13 (2022) 1–19, https://doi.org/10.3389/fimmu.2022.866747.
[76] Z. Chen, K.A. Vallega, H. Chen, J. Zhou, S.S. Ramalingam, S.Y. Sun, The natural product berberine synergizes with osimertinib preferentially against MET-amplified osimertinib-resistant lung cancer via direct MET inhibition, Pharmacol. Res. 175 (2022), 105998, https://doi.org/10.1016/j.phrs.2021.105998.
[77] G.H. Xiao, M. Jeffers, A. Bellacosa, Y. Mitsuuchi, G.F. Vande Woude, J.R. Testa, Anti-apoptotic signaling by hepatocyte growth factor/Met via the phosphatidylinositol 3-kinase/Akt and mitogen-activated protein kinase pathways, Proc. Natl. Acad. Sci. U. S. A. 98 (2001) 247–252, https://doi.org/10.1073/pnas.98.1.247.
[78] A. Mantovani, S.K. Biswas, M.R. Galdiero, A. Sica, M. Locati, Macrophage plasticity and polarization in tissue repair and remodelling, J. Pathol. 229 (2013) 176–185, https://doi.org/10.1002/path.4133.
[79] M. Moransard, M. Sawitzky, A. Fontana, T. Suter, Expression of the HGF receptor c-met by macrophages in experimental autoimmune encephalomyelitis, Glia 58 (2010) 559–571, https://doi.org/10.1002/glia.20945.
[80] A.A. Arif, Y.H. Huang, S.A. Freeman, J. Atif, P. Dean, J.C.Y. Lai, M.R. Blanchet, K. C. Wiegand, K.M. McNagny, T.M. Underhill, M.R. Gold, P. Johnson, C.D. Roskelley, Inflammation-induced metastatic colonization of the lung is facilitated by

hepatocyte growth factor-secreting monocyte-derived macrophages, Mol. Cancer Res 19 (2021) 2096–2109, https://doi.org/10.1158/1541-7786.MCR-21-0009.
[81] V.E. Lorenc, R. Lima e Silva, S.F. Hackett, S.D. Fortmann, Y. Liu, P.A. Campochiaro, Hepatocyte growth factor is upregulated in ischemic retina and contributes to retinal vascular leakage and neovascularization, FASEB BioAdvances 2 (2020) 219–233, https://doi.org/10.1096/fba.2019-00074.
[82] N. Nishikoba, K. Kumagai, S. Kanmura, Y. Nakamura, M. Ono, H. Eguchi, T. Kamibayashiyama, K. Oda, S. Mawatari, S. Tanoue, S. Hashimoto, H. Tsubouchi, A. Ido, HGF-MET signaling shifts M1 macrophages toward an M2-like phenotype through PI3K-mediated induction of arginase-1 expression, Front. Immunol. 11 (2020) 1–10, https://doi.org/10.3389/fimmu.2020.02135.
[83] W. Choi, J. Lee, J. Lee, S.H. Lee, S. Kim, Hepatocyte growth factor regulates macrophage transition to the M2 phenotype and promotes murine skeletal muscle regeneration, Front. Physiol. 10 (2019), https://doi.org/10.3389/fphys.2019.00914.
[84] S. Morioka, C. Maueröder, K.S. Ravichandran, Living on the Edge: Efferocytosis at the Interface of Homeostasis and Pathology, Immunity 50 (2019) 1149–1162, https://doi.org/10.1016/j.immuni.2019.04.018.
[85] D.A. Walsh, D.F. McWilliams, Mechanisms, impact and management of pain in rheumatoid arthritis, Nat. Rev. Rheumatol. 10 (2014) 581–592, https://doi.org/10.1038/nrrheum.2014.64.
[86] I. Galvão, J.P. Vago, L.C. Barroso, L.P. Tavares, C.M. Queiroz-Junior, V.V. Costa, F. S. Carneiro, T.P. Ferreira, P.M.R. Silva, F.A. Amaral, L.P. Sousa, M.M. Teixeira, Annexin A1 promotes timely resolution of inflammation in murine gout, Eur. J. Immunol. 47 (2017) 585–596, https://doi.org/10.1002/eji.201646551.